

Dynamic industry uncertainty networks and the business cycle*

Jozef Baruník¹, Mattia Bevilacqua², and Robert Faff³

¹Charles University and Czech Academy of Sciences

²Systemic Risk Centre, London School of Economics

³University of Queensland, Australia

Abstract

This paper introduces new forward-looking uncertainty network measures built from the main US industries. We argue that this network structure extracted from options investors' expectations is meaningfully dynamic and contains valuable information relevant for business cycles. Classifying industries according to their contribution to system-related uncertainty across business cycles, we uncover an uncertainty hub role for the communications, industrials and information technology sectors, while shocks to materials, real estate and utilities do not propagate strongly across the network. We find that a dynamic ex-ante network of uncertainty is a useful predictor of business cycles especially when it is based on uncertainty hubs. The uncertainty network is found to behave counter-cyclically since a tighter network of industry uncertainty tends to associate with future business cycle contractions.

Keywords: Financial Uncertainty, Industry Network, Options Market, Business Cycle.

*We thank Charlie Cai and Jacky Qi Zhang for their valuable comments. We thank the participants at the 3rd Workshop on Macroeconomic Research, Cracow University (September 2020, virtual) and CFE 2020 (December 2020, virtual). Mattia Bevilacqua gratefully acknowledges the support of the Economic and Social Research Council (ESRC) in funding the Systemic Risk Centre [grant number ES/K002309/1 and ES/R009724/1]. Jozef Baruník gratefully acknowledges support from the Czech Science Foundation under the EXPRO GX19-28231X project.

1 Introduction

Throughout history, industrial structure in developed economies has witnessed prominent influential economic and financial cycles in which different sectors seem to take on a leading role.¹ Fluctuations in performance, valuation and interconnection have been crucially important not only for swings in financial markets, but also for the real economy and the prediction of business cycles. Given this backdrop, we develop a forward-looking and dynamic measure of industry uncertainty network connectedness, we link this connectedness measure to the US economy and its importance in better understanding how aggregate economic activity is driven by the nuanced interrelations between economic sectors.

Understanding the differential actions and performance of the largest firms within an economy’s various industrial sectors offers key insight into the aggregate economy.² Many economic fluctuations are attributable to the incompressible “grains” of economic activity, stemming from individual companies (see [Gabaix, 2011](#)). Moreover, [Acemoglu et al. \(2012\)](#) documented that significant aggregate fluctuations can plausibly originate from firm-specific microeconomic shocks or disaggregated sectors due to interconnections between different firms and sectors, functioning as a potential propagation mechanism of idiosyncratic shocks throughout the economy. Further, [Carvalho and Gabaix \(2013\)](#) argue that the sector-specific “fundamental” microeconomic volatility has explanatory power and can serve as an early warning signal of swings in macroeconomic volatility. Notably, [Atalay \(2017\)](#) concludes that 83% of the variation in aggregate output growth is attributable to idiosyncratic industry-level shocks, while [Gabaix \(2011\)](#) contends that a salient feature of business cycles is that firms and sectors comove.

Industrial network connectedness has been evolving, sometimes strengthening and other

¹The ascendancy of technology and telecommunications is a notable recent example. The rapidly growing internet sector accounted for \$2.1 trillion of the U.S. economy in 2018 or about 10% of the nation’s gross domestic product (GDP). Tech companies such as Apple, Google, and Amazon are leading the stock market; any little variation in their quarterly earnings or stock market prices can move the entire index.

²For example, [Gabaix \(2011\)](#) reports that the total sales of the top 50 firms accounted for 25% of GDP in 2005. As another example, in December 2004, a \$24 billion one-time Microsoft dividend boosted growth in personal income from 0.6% to 3.7% (Bureau of Economic Analysis, January 31, 2005).

times weakening, across different time periods and at various points throughout economic cycles. We study the dynamic network concept from a fresh perspective, namely, through the lens of how industry-specific shocks to option buyers' expectations can propagate ex ante uncertainty. More specifically, we ask how does this form of network uncertainty develop over time and what is its relationship with the evolution of business activity, manifesting through business cycles?

To this end, we devise and construct a measure of ex-ante industry uncertainty network connectedness based on information extracted from options market data – data that reflects investor expectations of future uncertainty relevant to each industry. We study the dynamic relations of these uncertainty measures with the business cycle, characterizing each industry based on their expected contribution to shocks to uncertainty to the system across phases of the business cycle. Our analysis then quite naturally transitions to the question of how useful is this measure of network uncertainty in predicting business cycle phases.

Previous studies highlight the importance of network measures to capture the propagation of volatility mechanisms (e.g. [Acemoglu et al., 2012](#); [Carvalho and Gabaix, 2013](#); [Gabaix, 2016](#); [Barrot and Sauvagnat, 2016](#); [Acemoglu et al., 2017](#); [Baqae and Farhi, 2019](#); [Herskovic et al., 2020](#)). For example, measuring network effects is crucial to explain the joint evolution of firm volatility distributions (see [Herskovic et al., 2020](#)). Notably, the survey in [Carvalho and Tahbaz-Salehi \(2019\)](#) entreats researchers to develop models that take such firm-level forces seriously – in the belief that such efforts hold the key to capturing valuable theoretical and empirical richness that is currently missing from the literature. Put simply, our paper is answering this call to action at the industry level.

Fluctuations in risk are the most important shock driving the business cycle (see [Christiano et al., 2014](#)). According to [Bloom et al. \(2018\)](#), uncertainty is an important factor in business cycles, it is strongly countercyclical, this being true both at the aggregate and the industry level. We augment this existing literature by assessing the propagation of forward-looking industry-specific shocks in uncertainty and the way in which the aggregate

network extracted from the idiosyncratic shocks propagate dynamically; and to what extent significant aggregate fluctuations can originate from such shocks.

Previous literature on uncertainty and the related network measures relies on historical or ex post analysis. We contend that such backward-looking approaches are inferior to a forward-looking, ex ante, approach that employs measures extracted from option prices of individual firms. Accordingly, we construct a novel option-based uncertainty measure for each major company, spread across 11 US industries. We create aggregate uncertainty measures for each industry in our sample, covering 20 years at the daily frequency, with three recession periods, including the most recent Covid-19 crisis.

We characterize shocks at the industry uncertainty level and study their propagation mechanism across time. To do this, we adopt the dynamic network measures based on time-varying parameter VAR (TVP VAR) models introduced by [Barunik and Ellington \(2020\)](#). This technique estimates the adjacency matrix characterizing a network at each point in time using the variance decomposition matrix. They have a direct causal interpretation that permits the understanding of how shocks to uncertainty create dynamic networks among industry uncertainties, and are thereby useful for various macroeconomic applications e.g. characterizing the propagation of such networks over phases of the business cycle.³

The essential contribution of our work lies at the intersection of two relatively recent strands of literature. The first strand is on uncertainty measures (e.g. [Bloom, 2009](#); [Jurado et al., 2015](#); [Ludvigson et al., 2020](#)) to cite but a few; see also [Bloom \(2014\)](#) for a survey, and especially on the relationship between uncertainty and business cycle fluctuations that began with the work of [Bloom \(2009\)](#).⁴ Some of these studies assess how exogenous changes in volatility are key to generating business cycles and also analyze the possibility of reverse causation between measured uncertainty and business cycles.

The second strand includes studies on the role of sector-level or firm-to-firm linkages in

³Our approach is intimately connected to network node degrees, mean degrees, and connectedness measures of [Diebold and Yilmaz \(2012\)](#) and [Diebold and Yilmaz \(2014\)](#).

⁴See also [Bachmann et al. \(2013\)](#), [Bachmann and Bayer \(2014\)](#), [Christiano et al. \(2014\)](#), [Decker et al. \(2016\)](#), [Bloom et al. \(2018\)](#), and [Arellano et al. \(2019\)](#).

microeconomic shocks and their relationship with the aggregate economy, future economic downturns and changes in business conditions (see, e.g. [Acemoglu et al., 2012, 2017](#); [Baqae and Farhi, 2019](#)) or the survey in [Carvalho and Tahbaz-Salehi \(2019\)](#). Connected to this strand of literature, are studies on the role of production networks as a propagation mechanism from individual firms and/or industries to the real economy (e.g. [Di Giovanni et al., 2014](#); [Ozdagli and Weber, 2017](#); [Carvalho and Tahbaz-Salehi, 2019](#); [Auer et al., 2019](#); [Lehn and Winberry, 2020](#)). In contrast to these latter works, we adopt pure financial market based networks as a mechanism to study the propagation of shocks to uncertainty from industries to the real economy.

To the best of our knowledge, we are the first to propose an ex ante industry-based uncertainty network measure containing market participant expectations about forward-looking (next month) industry uncertainty and relate it to business cycles. Being able to temporally and precisely characterize these industry-based network dynamics is important given that industries can swiftly change their characteristics and macro-economic roles.⁵

The technological and housing market bubbles, the commodity crash, and the Covid pandemic are a few major examples that show how a dramatic increase in uncertainty and different investor expectations can rise sharply in many alternative industries. Through a TVP-VAR model, industries are more precisely assessed as to their contribution to shocks in uncertainty to the whole system across different phases of the business cycle, shedding crucial light on their mutating interactions and roles.

We identify industries showing a stronger (versus weaker) contribution of shocks to uncertainty, thus playing an essential role within the aggregate industry uncertainty network. [Lehn and Winberry \(2020\)](#) show that the empirical network is dominated by a few “investment hubs” that produce the majority of investment goods, are highly volatile, and are strongly correlated with the cycle. Similarly, and augmenting the definition of “hubs”

⁵[Pástor and Veronesi \(2009\)](#) show that stock prices rise with higher uncertainty during times of technological revolutions. The idea that have seen the financial sector always at the top of this pyramid is slightly mutating. On the importance of industry factors and industry risk see especially [Griffin and Karolyi \(1998\)](#), [Griffin and Stulz \(2001\)](#), [Griffin et al. \(2003\)](#) and [Carriero et al. \(2004\)](#).

in the input-output network literature, we characterize critical “uncertainty hubs”, as industries that largely transmit and/or receive uncertainty across the business cycle, versus “non-hubs”, being those industries that are (largely) neutral across business cycles.

When performance varies across industries, especially when the currently most influential ones are affected, this can trigger major consequences for the other industries, tightening or weakening the uncertainty network and being ultimately reflected in the real economy. Therefore, we also investigate whether the ex-ante industry-based uncertainty network might translate uncertainty shocks at the industry-based microeconomic level into fluctuations in macroeconomic aggregates (e.g. [Gabaix, 2011](#); [Acemoglu et al., 2012](#); [Carvalho and Gabaix, 2013](#); [Barrot and Sauvagnat, 2016](#); [Atalay, 2017](#)). To this end, we empirically test whether the aggregate ex ante uncertainty industry network is able to predict business cycles, hypothesizing enhanced predictive ability given that it is built on forward looking option information and through precise time-varying parametrization. We further hypothesize that the industry network constructed from uncertainty hubs achieve greater predictability compared to uncertainty in the non-hubs network.

The main findings of our paper are as follows. We find that the ex ante industry network is countercyclical and rises sharply during the dot com bubble, the global financial crisis (GFC), increasing steadily afterwards. The communications and information technology uncertainty networks play a key role, being classified as the main uncertainty hubs. In contrast, materials, utility and real estate are classified as non-hubs. Notably, the financial industry reveals a key role mainly during the GFC, while other industries are found to be time-varying uncertainty hubs according to specific business cycle phases (e.g. Covid-19 recession). Our empirical exercise shows the usefulness of the ex ante uncertainty network in predicting business cycles up to one year horizons. The results are robust with regard to several checks and the inclusion of additional control variables. Finally, we find that the uncertainty hubs network show greater predictive power with respect to business cycles, compared to their non-hub counterparts.

The remainder of this paper is organized as follows. Section 2 describes the data and sampling used in our study. Section 3 sets out the essence of the TVP-VAR network connectedness method applied to our chosen industry setting. Section 4 studies the dynamic aggregate uncertainty network connectedness, and section 5 presents the findings with respect to the dynamic idiosyncratic uncertainty network connectedness through the business cycle. Section 6 studies the predictive ability of the networks for the real economy. Section 7 concludes the paper. Additional results are relegated to the appendix of the paper.

2 Industry uncertainty, investor beliefs and option prices

To study the dynamic uncertainty network, we develop a forward-looking measure reflecting investor beliefs derived from option price data. To track investor’s beliefs and to allow trading on forward-looking volatility, the Chicago Board Options Exchange (CBOE) introduced a volatility index – VIX – extracting expectations from options prices in a model-free manner. The concept was later formalized by Bakshi and Madan (2000); Bakshi et al. (2003) and has quickly gained popularity in the literature as well as among practitioners and policymakers.

To capture industry uncertainty, we use forward-looking uncertainty measures that are intimately related to the VIX methodology. However, rather than looking at the whole U.S. stock market, we measure uncertainty at the industry level, focusing on the main U.S. industries. Options-based measures of risk are superior to historical volatility measures with respect to both predictive power and set of information they encompass (e.g. Christensen and Prabhala, 1998; Santa-Clara and Yan, 2010; Baruník et al., 2020).

2.1 Extracting model-free industry uncertainty from option prices

For each chosen company, we compute a model-free implied volatility index as detailed in the Appendix, section B. This measure reflects expectations about investor uncertainty with respect to the individual company over the coming 30 day horizon. We then aggregate the

individual company information to construct a measure of ex ante uncertainty at the industry level. Such measure reflects the industry expected uncertainty over the next 30 days.

More formally, the ex ante industry uncertainty measure $IVIX_t^{(\text{Ind})}$ is constructed by taking the time-varying weighted average of the main five stocks in each industry and at each point in time through our sample period as:

$$IVIX_t^{(\text{Ind})} = \sum_{s \in N^{(\text{Ind})}} \mathcal{W}_t^{(s)} VIX_t^{(s)} \quad (1)$$

where $\text{Ind} \in \{1, \dots, 11\}$ represents the industry we consider, s is an index for one of the $N^{(\text{Ind})}$ companies included in the given industry at time t , $VIX_t^{(s)}$ is an implied volatility for an individual stock s , and $\mathcal{W}_t^{(s)}$ is the time-varying market capitalization weight of that specific stock s computed as the ratio between the time-varying market capitalization of the stock and total market capitalization of all stocks included in the industry.

2.2 Data

We use daily data encompassing the sample period January 2000 to May 2020⁶ in each of the following 11 US industries: consumer discretionary (CD), communications (CM), consumer staples (CS), energy (E), financial (F), health care (HC), industrial (IN), information technology (IT), materials (M), real estate (RE) and utilities (U).⁷ More specifically we merge two data sources. We use options data from OptionMetrics from January 2000 to December 2018 to compute the individual stock VIXs. We expand the coverage of VIX time series from January 2019 until May 2020 aided by the IHS Markit’s Totem Vanilla Volatility Swap data

⁶Prior to 2000, there are insufficient available data to compute the individual stock VIX.

⁷The new communication service sector of the S&P 500 includes now big companies such as Facebook and Alphabet Google since these were moved out from the technology and consumer discretionary sectors, respectively, due to the changes of the Global Industry Classification Standard (GICS). The telecom sector changed its weight from about 2% of the entire S&P 500 to about 11%. The IT sector changes from a roughly 26% to about 20%; the consumer discretionary dropped from 13% to about 11%. The communication sector, still includes existing telecom companies such as Verizon Communications Inc, AT&T Inc. Apple Inc remained in the IT sector, while Amazon remained in the CD sector.

set.⁸ From the latter, we collect broker-dealers consensus prices with respect to the volatility strike of the swaps. This aids our data collection since they are exactly the measures of individual company uncertainty, namely the individual stock VIXs, we are interested in, therefore allowing us to expand the data frame of this study.⁹ Overall, our data set includes options prices with respect to 69 US firms. We select the largest stocks in each US industry based on market capitalization and included in the *S&P500* index.¹⁰ The selected stocks account for more than 58% of the U.S. *S&P500* market capitalization, thus being a valid proxy for the 11 US industries, and being representative of a not trivial fraction of the US GDP (e.g. [Gabaix, 2011](#)). A large representation of the US stock market and its industries is what matters when studying these as economic and business cycle drivers.¹¹ Table A1 in the appendix shows the included stocks within each industry and their available time period. The other financial information such as market capitalization and trading volume regarding the selected stocks are collected from Bloomberg.

We roll the constituent stocks of every industry at every point in time according to time-varying market capitalizations, new IPOs, exclusions of the stocks from the *S&P500*, or missing data. Figure A1 in the appendix depicts an example of individual company uncertainty indexes.¹² In cases where options on a specific company have been only issued

⁸The Totem database is a service within IHS Markit that gathers a large variety of derivatives marks from the major broker-dealers and returns consensus prices after having checked for outliers and errors. In the volatility swaps service contributors are requested to price the volatility strike at which the swap would have an inception price of zero which should be the traders best estimate of mid-market. Before 2019 January, the majority of the data in the Totem Vanilla Volatility (or Variance) Swap services were monthly, therefore would have not served our purpose.

⁹This relationship has also been widely discussed in the literature, see for example [Carr and Wu \(2006\)](#) who provide an excellent history of the VIX index and [Carr and Lee \(2009\)](#) document a history of the development of the variance swap market. Moreover, [Filipović et al. \(2016\)](#) affirm that absent index jumps, the CBOE VIX index is the 30-day variance swap rate on the *S&P500* quoted in volatility units. [Cheng \(2019\)](#) state that the squared VIX at the 30-day horizon, under the assumption of no jumps, equals the 30-day realized variance in the *S&P500* starting from date t . Thus, the squared VIX equals the fair strike on a variance swap. Consequently, the VIX equals the strike of a volatility swap.

¹⁰For example, these do not include Tesla, Royal Dutch Shell or Unilever.

¹¹[Gabaix \(2011\)](#) states that macroeconomic questions can be clarified by looking at the behavior of large firms. He adopts a sample including annual US Compustat data for the largest 100 firms as of 2007.

¹²The CBOE has introduced stock market VIX series for a few stocks in the US. Comparing our calculations, with available period CBOE counterparts, show a correlation, on average, exceeding 94%. This minor divergence is likely due to the interpolation among the two closest expiration dates to 30 days used in the CBOE methodology. For the data collected by IHS Markit spanning a shorter time frame, the correlation

in recent times, we include the next ranked company as a substitute, so as to always ensure at least five stocks for every sector across our time period.¹³ in that industry with available data.¹⁴ We report the descriptive statistics for the industry uncertainty indexes in Table 1.

Table 1: Industry Uncertainty $IVIX_t^{(Ind)}$ Descriptive Statistics

Ind	CD	CM	CS	E	F	HC	IN	IT	M	RE	U
Mean	0.321	0.318	0.230	0.270	0.370	0.252	0.300	0.342	0.289	0.343	0.232
Standard Dev.	0.116	0.121	0.096	0.106	0.279	0.089	0.148	0.144	0.111	0.191	0.107
Min	0.133	0.1305	0.115	0.128	0.145	0.136	0.139	0.138	0.152	0.122	0.104
Max	0.876	1.137	0.911	1.404	2.682	0.815	1.409	0.994	1.191	2.225	1.018
Skewness	1.363	1.538	1.777	3.249	3.727	1.552	2.409	1.504	2.220	2.769	2.246
Kurtosis	4.658	5.755	6.363	21.240	20.468	5.969	11.411	5.011	11.247	17.057	9.788

Notes: This table reports the descriptive statistics for the industry uncertainty $IVIX_t^{(Ind)}$ index of 11 industries: consumer discretionary (CD), communications (CM), consumer staples (CS), energy (E), financial (F), health care (HC), industrial (IN), information technology (IT), materials (M), real estate (RE) and utilities (U). The time period is from 03-01-2000 to 29-05-2020, at daily frequency.

From Table 1 we observe that the financial industry uncertainty shows the highest mean, followed by the information technology and real estate industry uncertainty measures with consumer staples and utilities showing the lowest mean values. The financial sector is also found to be the one with the highest standard deviation, and skewness of uncertainty measure. On the other hand, consumer staples, energy, health care and utilities are found to have lower standard deviations. Consumer discretionary and information technology show lower skewness and kurtosis compared to the other industries uncertainty measures. The minimum values of industry uncertainty range between 10% and 15%, while the maximum values present a wider range with financial and real estate leading with the highest values. As an example, we plot uncertainty measures for information technology, consumer staples

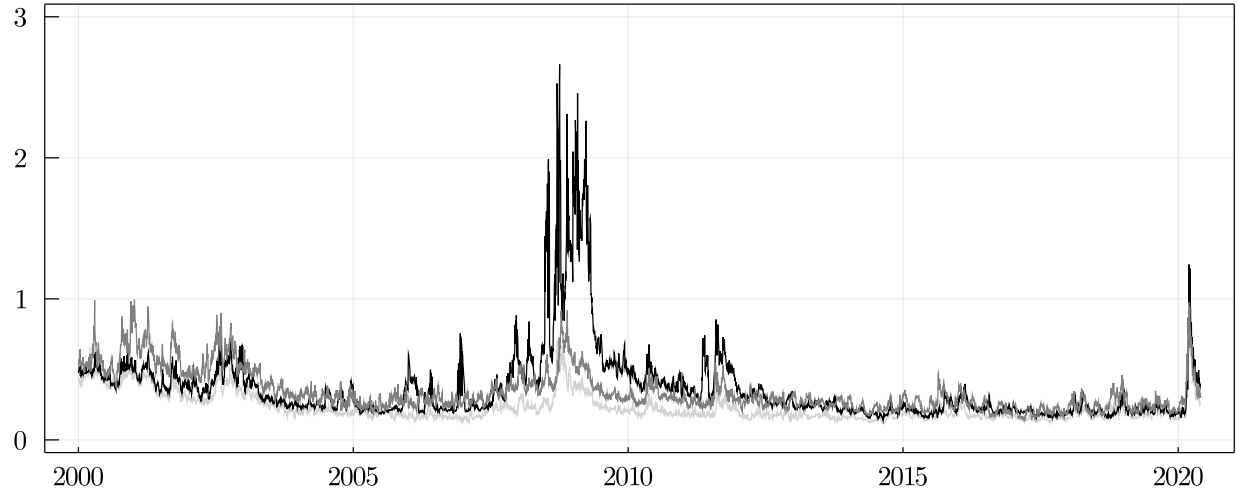
between the consensus volatility and CBOE VIX series is, on average, above 97%, this again due to the interpolation used in the CBOE methodology.

¹³The only exceptions are the materials and real estate industries. For the first we use only four stocks, monthly interpolated between 01-2019 and 04-2019 due to data availability. This is because before 05-2019 for a few stocks in this sector the submission service was monthly. Between 01- and 04-2019 no single firm volatility data is available for the real estate industry. We replace $IVIX_t^{(RE)}$ directly with the real estate sector volatility measure submitted to IHS Markit/Totem.

¹⁴With respect to some industries such as industrial, the same five stocks have been adopted throughout the sample period. In more dynamic sectors such as information technology, we observe several changes in the stocks ranking within our sample period ending up with GOOG, MSCF, INTEL, AAPL in the last decade.

and financial sector in Figure 1.

Figure 1: **Industry Uncertainty**



Notes: This figure shows $IVIX_t^{(Ind)}$ series for financial (black), information technology (grey) and consumer staples (light grey) covering the period 03-01-2000 to 29-05-2020 at a daily frequency.

We observe that the IT sector dominates the other two during the dot com bubble and technologic boom in the early 2000s. The financial sector shows predominant series during the GFC in 2008 and the Eurozone debt crisis in 2010 and 2011. In the most recent times, the IT sector exhibits greater uncertainty in comparison to the financial sector, showing how uncertainty might come from the innovation in technology. Consumer staples show peaks in the early 2000s and during the 2008 financial crisis, however being always below the other two series and overall quite low throughout our sample period. All three selected indexes spiked in correspondence to the recent Covid-19 outbreak in March 2020. Among them, we observe that financial and information technology increased during the Covid-19 crisis in a more pronounced manner compared to consumer staples, impacted less by the Covid-19 crisis.

3 Measurement of dynamic industry-level networks of uncertainty

Industries are connected directly through counterparty risk, contractual obligations or other general business conditions of the companies. High-frequency analysis of such networks requires generally unavailable high-frequency information. In contrast, option prices and uncertainty measured in high frequencies reflect the decisions of many agents assessing risks from the existing linkages. Hence the pure market-based approach we use in contrast to other network techniques allows us to monitor the network on a daily frequency as well as to exploit its forward-looking strength with minimal assumptions.

Looking at how a shock to the expected uncertainty of a company j transmits to future expectations about the uncertainty of a company k , we will define weighted and directed networks. Aggregating the information about such networks can provide industry level uncertainty characteristics that will measure how strongly the investors' expectations are interconnected. Importantly, we will focus on the time variation of such networks.

3.1 Link to the network literature and causality of proposed measures

The measures that we use are intimately related to modern network theory. Algebraically, the adjacency matrix capturing information about network linkages carries all information about the network, and any sensible measure must be related to it. As noted by [Diebold and Yilmaz \(2014\)](#), a variance decomposition matrix defining network adjacency matrix is then readily used as a network connectedness that is related to network node degrees and mean degree. Currently studies examine, almost exclusively, static networks mimicking time dynamics with estimation from an approximating window. In contrast to this approach, we follow [Barunik and Ellington \(2020\)](#) who employ a locally stationary TVP VAR that allows us to estimate the adjacency matrix for a network at each point in time with possibly large

dimension. Dynamic networks defined by such time-varying variance decompositions are then more sophisticated than classical network structures in several ways.

In a typical network, the adjacency matrix contains a set of zero and one entries, depending on the node being linked or not, respectively. In the above notion, one interprets variance decompositions as weighted links showing the strength of the connections. In addition, the links are directed, meaning that the j to k link is not necessarily the same as the k to j link, and hence, the adjacency matrix is not symmetric. Therefore we can define weighted, directed versions of network connectedness statistics readily that include degrees, degree distributions, distances and diameters. Using the time-varying approximating model, we will define a truly time-varying adjacency matrix that will describe a dynamic network.

The network connectedness measure we propose is also directly connected to the vast economic network literature in relation to production networks and granular shocks (see [Acemoglu et al., 2012](#); [Carvalho and Gabaix, 2013](#); [Gabaix, 2016](#); [Barrot and Sauvagnat, 2016](#); [Acemoglu et al., 2017](#); [Baqaee and Farhi, 2019](#); [Acemoglu and Azar, 2020](#)). The network analysis has developed a conceptual framework and an extensive set of tools to effectively measure interconnections among the units of analysis comprising a network, see for instance the survey paper by ([Carvalho and Tahbaz-Salehi, 2019](#)).

Moreover, our network connectedness measure improves on shocks to uncertainty measured ex post (e.g. [Diebold and Yilmaz, 2014](#)). Employing implied measures of uncertainty gives one access to a different set of information in uncertainty reflecting market participants' expectations of future movements in the underlying asset, a set of information found superior compared to ex post measures of uncertainty (see [Christensen and Prabhala, 1998](#)). We are naturally interested in capturing shocks to the ex ante uncertainty of industry j that will transmit to future expectations about the uncertainty of industry k .¹⁵

Finally, we note that our measures can have a direct causal interpretation. [Rambachan](#)

¹⁵[Baruník et al. \(2020\)](#) stated that option based measures of uncertainty reflect decisions of many agents assessing the risks from the existing linkages. The options market-based approach allows us to monitor the network on daily frequency as well as use its forward looking strength in contrast to other network techniques based on balance sheet and other information which is generally unavailable at high frequency.

and Shephard (2019) provide an important discussion about causal interpretation of impulse response analysis in the time series literature. In particular, they argue that if an observable time series is shown to be a potential outcome time series, then generalized impulse response functions have a direct causal interpretation. Potential outcome series describe at time t the output for a particular path of treatments.

In the context of our study, paths of treatments are shocks. The assumptions required for a potential outcome series are natural and intuitive for a typical economic and/or financial time series: i) they depend only on past and current shocks; ii) series are outcomes of shocks; and iii) assignment of shocks depend only on past outcomes and shocks. The dynamic adjacency matrix we introduce in the next section is a transformation of generalized impulse response functions. Therefore, the dynamic adjacency matrix and all measures that stem from manipulations of its elements possess a causal interpretation; thus establishing the notion of causal dynamic network measures.

3.2 Construction of dynamic uncertainty network

To formalize the discussion, we construct a dynamic uncertainty network of industries from the industry implied volatilities computed for the main US industries and we interpret the TVP-VAR model approximating its dynamics as a dynamic network following the work of Barunik and Ellington (2020). In particular, consider a locally stationary TVP-VAR of lag order p describing the dynamics of industry uncertainty as

$$\mathbf{IVIX}_{t,T} = \Phi_1(t/T)\mathbf{IVIX}_{t-1,T} + \dots + \Phi_p(t/T)\mathbf{IVIX}_{t-p,T} + \epsilon_{t,T}, \quad (2)$$

where $\mathbf{IVIX}_{t,T} = \left(\text{IVIX}_{t,T}^{(1)}, \dots, \text{IVIX}_{t,T}^{(N)} \right)^\top$ is a doubly indexed N -variate time series of industry uncertainties, $\epsilon_{t,T} = \sum^{-1/2}(t/T)\eta_{t,T}$ with $\eta_{t,T} \sim NID(0, I_M)$, and $\Phi(t/T) = \left(\Phi_1(t/T), \dots, \Phi_p(t/T) \right)^\top$ are the time varying autoregressive coefficients. Note that t refers to a discrete time index $1 \leq t \leq T$ and T is an additional index indicating the sharpness of

the local approximation of the time series by a stationary one. Rescaling time such that the continuous parameter $u \approx t/T$ is a local approximation of the weakly stationary time-series (Dahlhaus, 1996), we approximate the $\mathbf{IVIX}_{t,T}$ in a neighborhood of a fixed time point $u_0 = t_0/T$ by a stationary process $\widetilde{\mathbf{IVIX}}_t(u_0)$ as

$$\widetilde{\mathbf{IVIX}}_t(u_0) = \Phi_1(u_0)\widetilde{\mathbf{IVIX}}_{t-1}(u_0) \dots + \Phi_p(u_0)\widetilde{\mathbf{IVIX}}_{t-p}(u_0) + \epsilon_t. \quad (3)$$

The process has time varying Vector Moving Average VMA(∞) representation (Dahlhaus et al., 2009; Roueff and Sanchez-Perez, 2016)

$$\mathbf{IVIX}_{t,T} = \sum_{h=-\infty}^{\infty} \Psi_{t,T,h} \epsilon_{t-h} \quad (4)$$

where parameter vector $\Psi_{t,T,h} \approx \Psi_h(t/T)$ is a time varying impulse response function characterized by a bounded stochastic process.¹⁶ The connectedness measures rely on variance decompositions, which are transformations of the information in $\Psi_{t,T,h}$ that permit the measurement of the contribution of shocks to the system. Since a shock to a variable in the model does not necessarily appear alone, an identification scheme is crucial in calculating variance decompositions. We adapt the generalized identification scheme in Pesaran and Shin (1998) to locally stationary processes.

The following proposition establishes a time-varying representation of the variance decomposition of shocks from asset j to asset k . It is central to the development of the dynamic network measures since it constitutes a dynamic adjacency matrix.

Proposition 1 (Dynamic Adjacency Matrix).¹⁷ *Suppose $\mathbf{IVIX}_{t,T}$ is a locally stationary process, then the time-varying generalized variance decomposition of the j th variable at a rescaled time $u = t_0/T$ due to shocks in the k th variable forming a dynamic adjacency*

¹⁶Since $\Psi_{t,T,h}$ contains an infinite number of lags, we approximate the moving average coefficients at $h = 1, \dots, H$ horizons.

¹⁷Note to notation: $[\mathbf{A}]_{j,k}$ denotes the j th row and k th column of matrix \mathbf{A} denoted in bold. $[\mathbf{A}]_j$, denotes the full j th row; this is similar for the columns. A $\sum A$, where A is a matrix that denotes the sum of all elements of the matrix A .

matrix of a network is

$$\left[\boldsymbol{\theta}^H(u)\right]_{j,k} = \frac{\sigma_{kk}^{-1} \sum_{h=0}^H \left(\left[\boldsymbol{\Psi}_h(u) \boldsymbol{\Sigma}(u) \right]_{j,k} \right)^2}{\sum_{h=0}^H \left[\boldsymbol{\Psi}_h(u) \boldsymbol{\Sigma}(u) \boldsymbol{\Psi}_h^\top(u) \right]_{j,j}} \quad (5)$$

where $\boldsymbol{\Psi}_h(u)$ is a time varying impulse response function.

Proof. See Appendix C. □

It is important to note that proposition 1 defines the dynamic network completely. Naturally, our adjacency matrix is filled with weighted links showing strengths of the connections over time. The links are directional, meaning that the j to k link is not necessarily the same as the k to j link. Therefore the adjacency matrix is asymmetric.

To characterize network uncertainty, we define total dynamic network connectedness measures in the spirit of Diebold and Yilmaz (2014); Barunik and Ellington (2020) as the ratio of the off-diagonal elements to the sum of the entire matrix

$$\mathcal{C}^H(u) = 100 \times \sum_{\substack{j,k=1 \\ j \neq k}}^N \left[\tilde{\boldsymbol{\theta}}^H(u) \right]_{j,k} / \sum_{j,k=1}^N \left[\tilde{\boldsymbol{\theta}}^H(u) \right]_{j,k} \quad (6)$$

where $\left[\tilde{\boldsymbol{\theta}}^H(u) \right]$ is a normalized $\boldsymbol{\theta}$ by the row sum. This measures the contribution of forecast error variance attributable to all shocks in the system, minus the contribution of own shocks. Similar to the aggregate network connectedness measure that infers the system-wide strengths of connections, we define measures that will reveal when an individual industry is a transmitter or a receiver of uncertainty shocks in the system. We use these measures to proxy dynamic network uncertainty. The dynamic directional connectedness that measures how much of each industry's j variance is due to shocks in other industry $j \neq k$ in the

economy is given by

$$\mathcal{C}_{j \leftarrow \bullet}^H(u) = 100 \times \sum_{\substack{k=1 \\ k \neq j}}^N [\tilde{\boldsymbol{\theta}}^H(u)]_{j,k} \bigg/ \sum_{j,k=1}^N [\tilde{\boldsymbol{\theta}}^H(u)]_{j,k}, \quad (7)$$

defining the so-called FROM connectedness. Note one can precisely interpret this quantity as dynamic from-degrees (or out-degrees in the network literature) that associates with the nodes of the weighted directed network we represent by the dynamic variance decomposition matrix. Likewise, the contribution of asset j to variances in other variables is

$$\mathcal{C}_{j \rightarrow \bullet}^H(u) = 100 \times \sum_{\substack{k=1 \\ k \neq j}}^N [\tilde{\boldsymbol{\theta}}^H(u)]_{k,j} \bigg/ \sum_{j,j=1}^N [\tilde{\boldsymbol{\theta}}^H(u)]_{k,j} \quad (8)$$

and is the so-called TO connectedness. Again, one precisely interprets this as dynamic to-degrees (or in-degrees in the network literature) that associates with the nodes of the weighted directed network that we represent by the variance decompositions matrix. These two measures show how other industries contribute to the uncertainty of industry j , and how industry j contributes to the uncertainty of others, respectively, in a time-varying fashion. Further, the NET dynamic connectedness showing whether an industry is inducing more uncertainty than it receives from other industries in the system can be calculated as the difference between TO and FROM is as $\mathcal{C}_{j,\text{NET}}^H(u) = \mathcal{C}_{j \rightarrow \bullet}^H(u) - \mathcal{C}_{j \leftarrow \bullet}^H(u)$ and the AGG connectedness measure as $\mathcal{C}_{j,\text{AGG}}^H(u) = \mathcal{C}_{j \rightarrow \bullet}^H(u) + \mathcal{C}_{j \leftarrow \bullet}^H(u)$.

Finally, to obtain the time-varying coefficient estimates, and the time-varying covariance matrices at a fixed time point $u = t_0/T$, $\boldsymbol{\Phi}_1(u), \dots, \boldsymbol{\Phi}_p(u)$ $\boldsymbol{\Sigma}(u)$, we estimate the approximating model in (2) using Quasi-Bayesian Local-Likelihood (QBLL) methods (Petrova, 2019).

Specifically, we use a kernel weighting function that provides larger weights to observations that surround the period whose coefficient and covariance matrices are of interest. Using conjugate priors, the (quasi) posterior distribution of the parameters of the model are available analytically. This alleviates the need to use a Markov Chain Monte Carlo

(MCMC) simulation algorithm and permits the use of parallel computing. Note also that in using (quasi) Bayesian estimation methods, we obtain a distribution of parameters that we use to construct network measures that provide confidence bands for inference. We detail the estimation algorithm in Appendix D.

4 A dynamic network connectedness of industry uncertainties

Working with a dynamic network estimates, we are able to characterize and time the events leading to more or less connected industry uncertainty providing new insights about the propagation of the ex-ante uncertainty shocks and identifying periods in which the US industries' uncertainty was tightly connected.

In tighter connectedness periods, a specific shock to an uncertainty with respect to any industry may generate an aggregate impact on the whole network of industries as well as on the real economy. We present the dynamic aggregate network connectedness in Figure 2. We identify several cycles mainly driven by key events that took place in our sample such as the dot com bubble in the early 2000s, the housing market bubble, the 2007-2009 GFC, and the most recent Covid-19 crisis. Some events might be described as bursts that rapidly subside, others might be characterized by a more continuous pattern and trend.

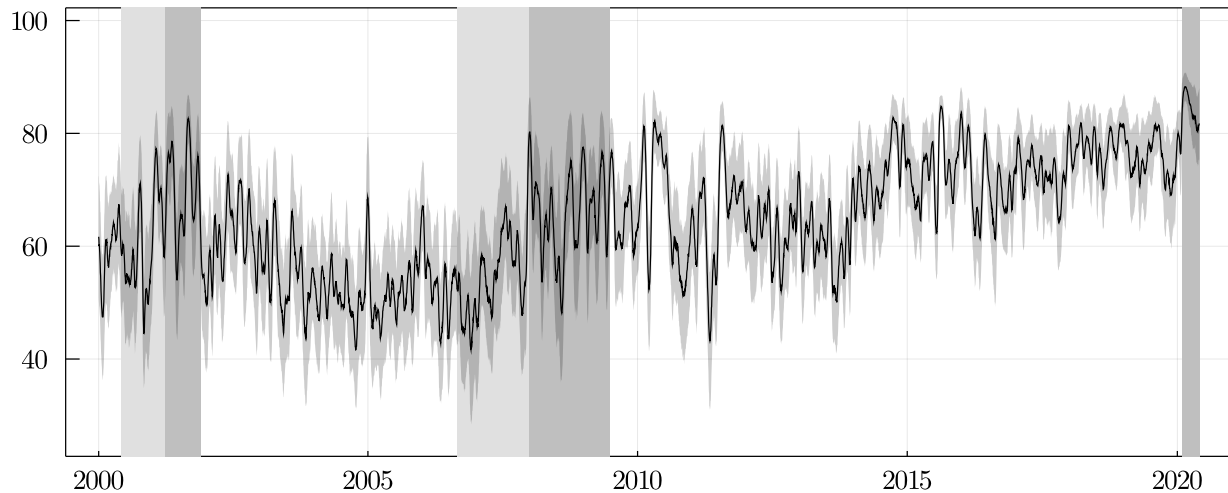
We also split the time period into inversions, recessions and expansions.¹⁸ Inversions are marked between July 2000 and March 2001 and between September 2006 and December 2007.¹⁹ The recessions are marked between April 2001 and November 2001, between January

¹⁸We follow the NBER classification, see <https://www.nber.org/cycles.html>.

¹⁹The FOMC raised the target fed funds rate by 25 basis points on June 29, 2006 and lowered the target by 50 basis points on September 18, 2007. Adrian and Estrella (2008) identified September 2006 as the end of the tightening cycle because during that month the one-month fed futures rate went from higher than the spot rate to lower. Due to the unprecedented causes of the pandemic recession in 2020, this has resulted in a downturn with different characteristics and dynamics than prior recessions (see NBER website). Hence, we are unable to establish an inversion period with respect to the Covid-19 crisis that we signal only as recession from February 2020.

2008 and June 2009, and between February 2020 until the end of the sample, while the other years are marked as expansions.

Figure 2: **Dynamic Network Connectedness of Industry Uncertainties**



Notes: This figure shows the dynamic uncertainty network connectedness with respect to the 11 US industries estimated during the 03-01-2000 – 29-05-2020 period at a daily frequency. Inversions (light grey area) are marked between July 2000 and March 2001 and between September 2006 and December 2007. The recessions (grey area) are marked between April 2001 and November 2001, between January 2008 and June 2009, and between February 2020 until the end of the sample, while the other years are marked as expansions. Note the network connectedness is plotted with two standard deviation percentiles of the measure.

We document the system to be strongly connected with values fluctuating around 60% in the first half of 2000. The first cycle starts with the burst of the tech bubble in 2000, and with the network measure climbing from about 60% to 68%, and increasing up to about 80% in the second half of 2001 as a response to the dot com bubble strengthening US industries' uncertainty connections via shock to uncertainty from the technology industry. The index recovers to the initial level until 2004, hitting minimum values in our sample at the end of 2004 before spiking again. After that, uncertainty network connectedness shows a new lower average level, fluctuating around 50% until the second half of 2007, the only exception being a peak at the end of 2005 which might be due to the US housing bubble showing a connectedness level up to 67%.

We observe the index recording a significant upward movement from the beginning of 2007 to 2009 reaching a level close to 80%, in response to the high uncertainty during the 2007–2009 GFC spreading from the financial industry to other industries. Several cycles can be detected during the 2007–2009 GFC: the first between the first quarter of 2007 and August 2007 reflecting the US credit crunch; the second in January–March 2008 (panic in stock and foreign exchange markets, and Bear Stearns’ takeover by JP Morgan), the collapse of the Lehman Brothers in September 2008 showing a spike from 47% to 75% in our network connectedness, and lastly in the first half of 2009 when the financial crisis started to propagate among all other industries, increasing the average network connectedness level.

Uncertainty connectedness spikes again in line with the two phases of the European sovereign debt crisis, in 2010 and in the second half of 2011, reaching one of the highest levels, up to that point, close to 80%. We then observe a drop in 2012, this being followed by a quite calm period from 2012 to mid-2013. Connectedness spikes again at the end of 2013 due to trade wars and energy turmoils reaching levels above 70%, and twice at the end of 2014 and in mid 2015 reaching its maximum level close up to that time, overcoming 80%. Connectedness peaks in correspondence of Brexit in 2016 and at the end of 2017, and eventually in 2020 due to the coronavirus outbreak, reaching its all time maximum value in March 2020 (a level of almost 90%), signalling the beginning of the Covid-19 crisis. This reflects the tight connectedness among all industries in the coronavirus period since almost all industries have been severely affected.

The fluctuations of the aggregate uncertainty network across crises, market downturns and expansions, and its countercyclical trend, open up for further investigation of the role of each uncertainty index. US industries appear to be more connected after the GFC and even more with the most recent Covid-19 crisis. We still lack understanding of which industries are driving such network increase or decrease with respect to different business cycles. The next sections aim to clarify these points exploiting the precise time varying estimation of the uncertainty network first, and its forward-looking properties in the last section.

5 Uncertainty networks across the business cycles

In addition to the aggregate network characteristics, we study how specific industries contribute to the ex-ante uncertainty of the system across the US business cycles and we classify them in the network. Specifically, we are interested to identify transmitters, receivers as well as industries being hubs of the uncertainty. We classify industries according to the $\mathcal{C}_{\text{NET}}^H$ and $\mathcal{C}_{\text{AGG}}^H$ characteristics of dynamic uncertainty network.

5.1 Hubs, non-hubs and business cycles

In the case of positive or negative NET measure an industry is deemed to be an uncertainty transmitter or receiver, respectively. An industry receiving or transmitting shocks to uncertainty with an intermediate level can be classified as a *moderate* transmitter or receiver, respectively, and may contribute to the uncertainty propagation in the system in a mild manner. An industry transmitting shocks to the system more (less) than receiving shocks from the system is labeled as a *transmitter* (*receiver*).

An industry showing high values of both directional measures reflected by high AGG values is playing an active role in transmission of uncertainty shocks and is denoted as “uncertainty hub”, being an industry that contributes the most to uncertainty shocks within the network. Conversely, a *neutral* industry showing low AGG values is denoted as “uncertainty non-hub”.

Industries might have changing roles in terms of contributors to shocks to uncertainty in relation to the specific economic cycle. We then average the network characteristics across each of the three business cycle phases (inversions, recessions and expansions) as described in the previous section, as well as over the total period. Table 2 provides the details.

Starting with inversion periods, F and IT industries are detected as the main hubs reflecting the role of these two industries in the dot com and GFC, respectively. A predominant role of these two industries in uncertainty network is also visible in the recession period. With the addition of the CD industry, all three are the main uncertainty hubs during recessions

playing a key role during the dot com, GFC and Covid-19 recessions. The IT industry is found to be a main uncertainty hub during all periods consistently, showing time-invariant role as a key industry with respect to the contribution of shocks to uncertainty, especially during the dot com and Covid-19 recessions. During expansion periods, CM also plays role in addition to the IT industry. In contrast, M, RE and U industries are detected to be uncertainty non-hubs, with the smallest values of network characteristics.

The total period uncovers IT, IN and CM industries as the main uncertainty hubs, with positive NET characteristics connected to highest AGG values. This finding highlights the important role such industries have played in the last two decades in the system. In addition, CD and E can also be classified as uncertainty hubs due to their high AGG statistics. Conversely, F, M, RE and U industries are uncertainty non-hubs within our sample. This finding shows how financial uncertainty has been transmitting differently across various times, mainly during inversions and recessions, but it is overall a non-hub.

Table 2: **Aggregate \mathcal{C}_{NET} and \mathcal{C}_{AGG} across business cycles**

	Inversion			Recession			Expansion			Total Period		
	NET	AGG	AGG %	NET	AGG	AGG %	NET	AGG	AGG %	NET	AGG	AGG %
CD	-1.72	16.77	9.8	0.49	35.02	10.9	-0.98	25.61	11.0	-0.71	29.61	11.1
CM	-1.55	13.07	7.6	-0.29	28.88	9.0	1.37	27.16	11.6	1.55	30.49	11.5
CS	-0.87	12.12	7.1	-0.15	32.70	10.2	-1.54	20.93	9.0	-1.50	24.27	9.1
E	-4.52	16.88	9.8	-0.43	30.70	9.5	-0.43	25.09	10.7	-0.80	28.27	10.6
F	3.76	21.07	12.3	0.01	40.55	12.6	0.04	18.02	7.7	0.54	22.15	8.3
HC	-0.76	14.23	8.3	-2.15	29.70	9.2	-0.29	23.63	10.1	-0.56	26.45	9.9
IN	0.92	20.63	12.1	-0.21	40.09	12.5	0.26	26.71	11.4	0.17	31.47	11.9
IT	4.42	25.09	14.7	2.77	39.74	12.4	1.93	28.48	12.2	2.23	33.71	12.7
M	-0.33	10.15	5.9	-1.77	15.99	5.0	-1.01	14.62	6.3	-0.98	15.84	6.0
RE	1.24	12.01	7.1	1.55	17.18	5.3	0.97	13.89	6.0	0.51	14.22	5.3
U	-0.58	9.11	5.3	0.19	11.04	3.4	-0.24	9.41	4.0	-0.43	9.59	3.6

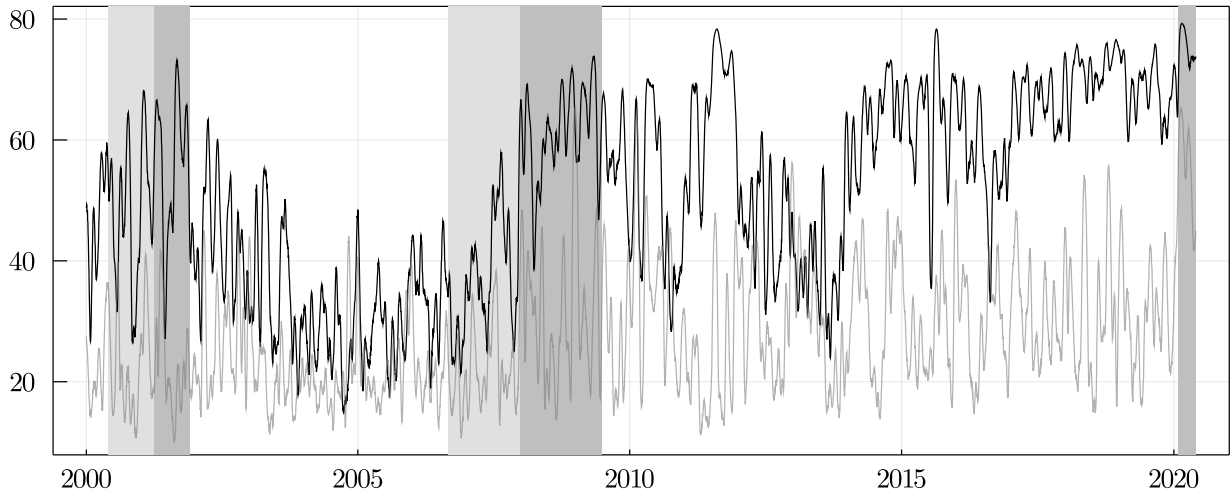
Notes: The table shows the average NET and AGG values with respect to the 11 U.S. industries' uncertainty network. When the NET measure is positive an industry can be classified as a NET marginal transmitter, while, when negative, it can be classified as a NET marginal receiver. The highest values of the AGG network statistics are associated with uncertainty hubs, while the lowest with uncertainty non-hubs. The statistics are reported for the business cycle main phases, namely inversion, recession, expansion, aggregated, and also for the total period, namely from 03-01-2000 to 29-05-2020, at a daily frequency.

Finally, industries classified as main uncertainty hubs in the sample are CD, CM, E, IN, and IT, whereas F, M, RE, and U are classified as non-hubs. Table 2 reveals that the IT industry is the main uncertainty hub contributing to the network connectedness characteristics two and three time larger in comparison to the M and U industries respectively. Industries

such as HC and CS are moderate contributors in our system.

After having classified the industries based on their contribution to uncertainty across business cycles, we compute separate networks of uncertainty hubs and non-hubs industries. Figure 3 plots dynamics of both network connectedness characteristics. We observe that the uncertainty network extracted from hubs shows a higher degree of integration compared to the ones extracted from non-hubs. This is especially evident after the GFC and in more recent years when uncertainty hubs such as CM, IN and IT have indeed played a key role contributing to shock in uncertainty within the system.

Figure 3: **Uncertainty Hubs and non-Hubs Networks**



Notes: This figure shows the network connectedness measures extracted from uncertainty hubs (black line) and non-hubs (grey line) from 03-01-2000 to 29-05-2020, at a daily frequency. Inversions (light grey area) are marked between July 2000 and March 2001 and between September 2006 and December 2007. The recessions (grey area) are marked between April 2001 and November 2001, between January 2008 and June 2009, and between February 2020 until the end of the sample, while the other years are marked as expansions.

5.2 Shocks to uncertainty in specific business cycles

We here briefly show a more granular classification of industries with respect to every business cycle across the whole time period investigating how industry uncertainty contributed to

shocks in each of the periods, since they share a very different nature. We report the \mathcal{C}_{NET} and \mathcal{C}_{AGG} statistics in Table F1 in appendix.

The IT industry can be classified as a main uncertainty hub during both inversion and recession phases related to the dot com bubble (from 2000 to mid-2002), contributing to spread uncertainty within the whole system. Given the high AGG values, CD and F are classified as main uncertainty hubs during the dot com recession. In contrast, M and U are classified as uncertainty non-hubs during this first recession.

Interestingly, around 2002-2004 we observe a role as uncertainty transmitters for RE since this period corresponds to the US housing market bubble. The 2007–2008 GFC was indeed related to the bursting of real estate bubbles, identified precisely by the dynamic network at the end of 2005. We observe a main role as uncertainty transmitter for F between 2006 and 2007 reflecting the first events related to the GFC and the mortgage crisis. The F industry spiked again transmitting uncertainty exactly in correspondence to the collapse of the Lehman Brothers in September 2008. It shows a predominant role as main NET transmitter during the GFC, both in inversion and actual recession, being therefore classifiable as a main uncertainty hub within this period, contributing to spread uncertainty within the whole system. Notably, during the GFC inversion, all the other industries are found to be mainly uncertainty non-hubs, either receiving uncertainty or being neutral to the upcoming recession, only exception being the IN industry.

The US economy is characterized by a long recovery period after this in which CM and IT are, by far, the main uncertainty hubs. The financial sector has seen one of the most-pronounced stock market booms on record during 2009-2018, this justifying the low level of uncertainty transmitted by F to the system. RE and U can be classified as uncertainty non-hubs. From 2010 until 2015 we observe a role as uncertainty hub for E, this could be due to a combination of events throughout this time period,²⁰ emphasized by the spike in

²⁰For instance the changes in the US energy policies, US conflicts in middle East, OPEC excessive production, and US oil prices collapse leading to higher oil price volatility. Moreover, in summer 2011, oil and other commodities prices have fallen, although from historically high levels, and this was reflected in the fear that the commodities boom was over, with raw materials set to drop sharply.

uncertainty between June 2014 and February 2015 associated with the global commodity price crash and oil price drop.

From 2015 until the end of our sample period, IN is found to be one of the main transmitters and uncertainty hubs within our system. Also CD, CM, and IT can be classified as uncertainty hubs in the same period, while all the other industries either as mild receivers or as uncertainty non-hubs. Finally, in the most recent Covid-19 recession, we notice that industries such as CD, CS, CM and IT are found to be the main uncertainty hubs, F the main net uncertainty receiver, while HC, RE, and U uncertainty non-hubs.

This analysis further highlights the usefulness of the time-varying parameters model to precisely uncover role of industries in shocks to uncertainty. Business cycles, economic downturns and crises with different nature may intensify the role of a specific industry, becoming such industry a key player in contributing to shocks to uncertainty within the network. It is then crucial to be able to identify the role of each industry across these times. Moreover, differences in terms of shocks to uncertainty might play a critical role in predicting business cycles throughout the sample.

6 Industry uncertainty networks and business cycle predictability

Information drawn from options and aggregated into ex ante uncertainty network may contribute to the predictability of indicators of business cycle. The main hypothesis drawn from the literature is that aggregated networks of *microeconomic* shocks to ex ante uncertainty may contribute to fluctuations in the macroeconomy activity and business cycles (e.g. [Gabaix, 2011](#); [Acemoglu et al., 2012](#); [Carvalho and Gabaix, 2013](#); [Barrot and Sauvagnat, 2016](#); [Atalay, 2017](#); [Lehn and Winberry, 2020](#)). Our network connectedness aggregates industry-level shocks from ex-ante uncertainty of companies within the same industry. The forward looking feature of the network is what we believe can be exploited to predict future

business cycles in advance. Furthermore, we argue that network extracted from uncertainty hubs play a more prevalent predictive role compared to the network extracted from uncertainty non-hubs with respect to future business cycles. The first may introduce some degree of innovation, compared to more neutral industries (non-hubs) thus possibly improving the prediction of future economic conditions.

The literature on business cycle indicators, turning points, expansions and recessions characterizations has a long history. The Business Cycle Dating Committee (BCDC) of the National Bureau of Economic Research (NBER) provides probably the large historical record of the economic activity classification and business cycles. However, its releases are usually made with about a year’s delay. It, therefore, represents a very reliable chronology of peaks and troughs throughout history rather than providing an early warning tool. The latter is what studies have been aiming to propose for decades. We study the relationship between uncertainty network connectedness and more timely indicators of business cycles, both coincident and leading indicators. We hypothesize that our network connectedness may represent an even more timely and forward looking predictor of business cycle indicators given its ex ante characteristics from the options market. It may therefore represent both a good predictor of coincident and leading indicators and it can be also classified as leading monitoring tool of business cycle itself. This would provide researchers, policy-makers and the public with a even more timely indicator than the ones already available.

6.1 The predictability of business cycle coincident indicators

[Berge and Jordà \(2011\)](#) provides an exhaustive summary of the different measures available that provide accurate signals about the current state of the business cycle. Among those there are the Chicago Fed National Activity Index (CFNAI) and the Aruoba, Diebold, and Scotti (ADS) index of business conditions. We adopt these as coincident indicators of business cycle and we study whether the uncertainty network is able to forecast them. Specifically, we adopt the 3-month moving average of the Chicago FED National Activity

Index (CFNAI-MA3) as well used proxy of business cycle.²¹ The Aruoba-Diebold-Scotti (ADS) Business Condition Index tracks real business conditions at a high frequency and it is based on economic indicators.²² We aggregate the ADS indicator at monthly frequency.

In addition, we disentangle our business cycles indicators into proxies for expansions and recessions following a more refined decomposition approach by [Berge and Jordà \(2011\)](#) who proposed optimal thresholds for CFNAI and ADS equal to -0.72 and -0.80, respectively. Thus, periods of economic expansion are associated with values of the CFNAI-MA3 above -0.72, whereas periods of economic contraction with values of the CFNAI-MA3 below -0.72. The same classification applies for ADS with respect to a -0.80 threshold. Aiming to study whether the predictive ability of the uncertainty network connectedness varies according to different states of the business cycle, we also investigate its predictability power with respect to either proxies of expansions or recessions as our dependent variables.

We aggregate network connectedness at a monthly frequency as to match the frequency of the business cycle indicators and we run the following predictive regression:

$$\mathcal{Y}_{t+h}^{(\ell)} = \beta_0 + \beta_C \mathcal{C}_t + \sum_{i=1}^N \beta_{X,i} X_{t,i} + \epsilon_t \quad (9)$$

where $\mathcal{Y}_{t+h}^{(\ell)}$ is one of the business cycle indicators we select (or their components) with the predictive horizon $h \in 1, 3, 6, 9, 12$ months. The \mathcal{C}_t is the industry uncertainty network connectedness measure (note we drop index H here for the ease of notation), $X_{t,i}$ is a set of control variables including both traditional predictors of business cycles such as oil

²¹The CFNAI is a monthly index that tracks the overall economic activity and the inflationary pressure. It is computed as the first principal component of 85 series drawn from four broad categories of data: 1) production and income (23 series), 2) employment, unemployment, and hours (24 series), 3) personal consumption and housing (15 series), and 4) sales, orders, and inventories (23 series). All of the data are adjusted for inflation. A zero value for the monthly index has been associated with the national economy expanding at its historical trend (average) rate of growth; negative values with below-average growth; positive values with above-average growth. For more information see <https://www.chicagofed.org/publications/cfnai/index>.

²²The average value of the ADS index is zero. Progressively positive values indicate progressively better-than-average conditions, whereas progressively more negative values indicate progressively worse-than-average conditions. It is collected from: <https://www.philadelphiafed.org/research-and-data/real-time-center>.

price changes (OIL), term spread as 10-year bond rate minus the 3-month bond rate (TS), unemployment rate (UR), (see also [Gabaix, 2011](#)), and also potential leading indicators extracted from the financial markets, namely the changes in the CBOE VIX index being a common proxy for uncertainty in the US (VIX), changes in the *S&P500* price index (SPX), the Bloomberg Commodity price index (COMM) and the S&P Case-Shiller Home price (CSHP).²³ Therefore, $X_{t,i}$ is indexed for i up to $N = 7$, the number of control we select, with $i \in (\text{OIL}, \text{TS}, \text{UR}, \text{VIX}, \text{SPX}, \text{COMM}, \text{CSHP})$.

Table 3 reports the results. With respect to the aggregate CFNAI-MA3 indicator of business cycle, we observe that uncertainty connectedness is a strong predictor of the business cycle up to 12 months in advance also after taking into account the information of the selected controls. The coefficient associated with our independent predictor is negative suggesting that a tighter network of industry uncertainties would lead to a contraction in the business cycle in the future horizons. The network is therefore found to behave counter-cyclically, a finding in line with previous studies relating uncertainty measures with the business cycles (e.g. [Bloom et al., 2018](#)). The performance of the models measured by the adjusted- R^2 is found to be close to 30% at the 1-month horizon, then it decreases at the semi-annual horizon, increasing again at longer horizons such as 9 and 12 months.

When we look at the disentangled components of the business cycle indicator, we observe that uncertainty network is able to predict well future expansion periods up to one year in advance. The sign associated with the models' coefficients is, again, negative therefore suggesting that expansion periods might contract when the network is tighter. Now we notice a greater adjusted- R^2 performance of the model with respect to 6- to 12-month horizons. Regarding US recession periods, we observe a weaker predictability of network across shorter horizons. However, uncertainty network is still found to predict well future recessions from 3-month up to 12-month horizon, being the higher adjusted- R^2 placed again on the longer

²³Oil prices, 10-year and 3-month bond rates, unemployment rate and the S&P Case-Shiller Home price index are collected from the Federal Reserve Bank of St. Louis economic database at <https://fred.stlouisfed.org/>; the CBOE VIX index, *S&P500* price index and the Bloomberg Commodity price index are collected from Bloomberg.

Table 3: CFNAI-MA3 Predictive Results

Panel A: CFNAI-MA3					
	$h=1$	$h=3$	$h=6$	$h=9$	$h=12$
$\mathcal{C}_t \mid X_t$	-0.013** (0.006)	-0.024*** (0.007)	-0.026*** (0.007)	-0.040*** (0.007)	-0.028*** (0.007)
Adj. R^2	0.294	0.156	0.067	0.176	0.168
Obs	243	241	238	235	232
Panel B: CFNAI-MA3 Expansion					
	$h=1$	$h=3$	$h=6$	$h=9$	$h=12$
$\mathcal{C}_t \mid X_t$	-0.007*** (0.002)	-0.010*** (0.002)	-0.012*** (0.002)	-0.011*** (0.002)	-0.008*** (0.002)
Adj. R^2	0.093	0.175	0.268	0.304	0.239
Obs	243	241	238	235	232
Panel C: CFNAI-MA3 Recession					
	$h=1$	$h=3$	$h=6$	$h=9$	$h=12$
$\mathcal{C}_t \mid X_t$	-0.006 (0.006)	-0.014** (0.007)	-0.013** (0.007)	-0.029*** (0.007)	-0.020*** (0.007)
Adj. R^2	0.287	0.135	0.059	0.144	0.148
Obs	243	241	238	235	232

Notes: This table presents the results of the predictive regression in equation 9 between the industry uncertainty network connectedness and the 3-month moving average of the Chicago FED National Activity Index (CFNAI-MA3), indicator of business cycle (Panel A). In Panel B and Panel C the results of the predictive regression with respect to the CFNAI-MA3 expansion and recession indicators are reported, respectively. We also add a set of controls, X . The five columns of the table represent different predictability horizons with $h \in (1, 3, 6, 9, 12)$. Regressions' coefficients and standard errors (in parentheses), and adjusted- R^2 are reported. Coefficients are marked with *, **, *** for 10%, 5%, 1% significance levels, respectively. Intercept and controls results are not reported for the sake of space. Series are considered at monthly frequency between 01-2000 and 05-2020.

horizon. Interestingly, we find a negative sign associated with the coefficients, this implying that increasing levels of network connectedness will expand the business cycle when in recession (in this case the dependent variable is below the -0.72 threshold, thus entering the regression with a negative sign).²⁴

We validate the predictive ability of uncertainty network connectedness by showing how it can also similarly predict a different coincident indicator of business cycle. We show the results with respect to the ADS Index in Table F1 in appendix. We observe that the aggregate uncertainty network measure shows predictability power with respect to the ADS index from 3 months up to 12 months in advance, with again negative coefficients and stronger performance at the long horizon. When we look at the expansion or recession

²⁴The Chicago Fed suggested -0.7 to be a more accurate threshold of turning points for the CFNAI indicator. We repeat the empirical analysis of this section by adopting this threshold. The results are found to be materially the same.

indicators, we find weaker predictive power at the short horizons, whereas strong predictive ability is still placed at longer horizons, especially with respect to the expansion indicator.

Another possible coincident indicator of business cycle can be the industrial production growth rate. As a robustness check, we repeat the same exercise with respect to the annualized growth rate of industrial production, still confirming the predictive ability of uncertainty network. We also adopt another business cycle coincident indicator collected from the Economic Cycle Research Institute (ECRI), the US coincident indicator (USCI).²⁵ We take the growth rate of the indicator and show that this leads to similar results, relegated to appendix in Table F2. As an additional robustness check, we also replace the uncertainty network connectedness measure constructed with time-varying networks with a network measure constructed by following previous studies (e.g. Diebold and Yilmaz, 2012; Diebold and Yilmaz, 2014) using moving window. We find that the latter is unable to predict future business cycles and the expansion and recession components, highlighting even more the importance of precisely characterizing the network at any point in time without relying on moving windows when it comes to predicting future levels of business cycle or the real economy.²⁶

6.2 Industry uncertainty networks and leading indicators

Due to its forward-looking nature, we argue that the uncertainty network connectedness may potentially also serve as a good predictor of leading indicators of business cycle, and be considered a leading indicator itself. We here check the predictive ability of this index with respect to two business cycle leading indicators: the US composite leading indicator (CLI) by the OECD.²⁷ and the US leading indicator (USLI) computed by the Economic Cycle Research Institute (ECRI).²⁸ USLI is available at weekly frequency and aggregated here at

²⁵For more information and data see <https://www.businesscycle.com/ecri-reports-indexes/all-indexes>.

²⁶The all set of results is available from the authors upon request.

²⁷The composite leading indicator is collected from the OECD data base at <https://data.oecd.org/leadind/composite-leading-indicator-cli.htm>. CLI provides early signals of turning points in business cycles showing fluctuation of the economic activity around its long term potential level.

²⁸For more information and data see <https://www.businesscycle.com/ecri-reports-indexes/all-indexes>.

monthly frequency, and we take the growth rate of the indicator. We find similar results, confirming both significance and coefficients signs, even after adding the set of controls. We repeat the same predictive exercise of the previous subsection, by running equation 9 where now the dependent variable is CLI. We report the results in Table 4. We observe that the predictability of uncertainty network connectedness is even stronger with respect to leading indicators of business cycle, spanning from 3-month up to one year and from 1-month up to 9-month horizons, with respect to CLI and USLI, respectively. The coefficients are still found to be negative confirming our previous findings.

Table 4: Leading Indicators Predictive Results

Panel A: CLI					
	$h=1$	$h=3$	$h=6$	$h=9$	$h=12$
$C_t X_t$	-0.011 (0.010)	-0.030*** (0.011)	-0.051*** (0.012)	-0.079*** (0.011)	-0.084*** (0.011)
Adj. R^2	0.435	0.294	0.192	0.247	0.262
Obs	243	241	238	235	232
Panel B: USLI					
	$h=1$	$h=3$	$h=6$	$h=9$	$h=12$
$C_t X_t$	-0.348*** (0.063)	-0.371*** (0.066)	-0.417*** (0.066)	-0.372*** (0.067)	-0.108 (0.073)
Adj. R^2	0.364	0.304	0.303	0.299	0.178
Obs	243	241	238	235	232

Notes: This table presents the results of the predictive regression in equation 9 between the industry uncertainty network connectedness and two leading indicators of business cycle, namely CLI and USLI, in Panel A and B, respectively. We also add a set of controls, X . The five columns of the table represent different predictability horizons with $h \in (1, 3, 6, 9, 12)$. Regressions' coefficients and standard errors (in parentheses), and adjusted- R^2 are reported. Coefficients are marked with *, **, *** for 10%, 5%, 1% significance levels, respectively. Intercept and controls results are not reported for the sake of space. Series are considered at monthly frequency between 01-2000 and 05-2020.

Overall, it appears that uncertainty network can anticipate what is commonly viewed as a leading indicator of business cycle. This opens up to some considerations. Given that the uncertainty network is extracted from options prices, it is expected that the newly proposed uncertainty network contains forward looking information that can be useful as ex ante business cycle monitoring indicator.

We know that a leading indicator of business cycle, as proposed by several papers and institutions, should ideally anticipate and predict coincident indicators. We showed in the

previous section that the uncertainty network shares such properties. In this subsection, we show how our network measure is also a good predictor of leading indicators, such a finding emphasizing even further the usefulness of its forward-looking information content.

In order to validate this point we test whether the existing leading indicators of business cycle may contain a different set of information, mainly at shorter horizons, compared to our uncertainty network. We test whether our measure can predict coincident indicators even after controlling for a leading indicator (CLI). The results are reported in Table 5.

Table 5: Coincident Indicators Predictive Results

Panel A: CFNAI-3M					
	$h=1$	$h=3$	$h=6$	$h=9$	$h=12$
$C_t X_t$	-0.011** (0.005)	-0.023*** (0.006)	-0.025*** (0.007)	-0.040*** (0.007)	-0.028*** (0.007)
CLI	0.432*** (0.036)	0.357*** (0.045)	0.265*** (0.051)	0.136*** (0.051)	0.008 (0.053)
Adj. R^2	0.560	0.333	0.162	0.198	0.164
Obs	243	241	238	235	232
Panel B: ADS					
	$h=1$	$h=3$	$h=6$	$h=9$	$h=12$
$C_t X_t$	-0.018 (0.015)	-0.026* (0.018)	-0.034* (0.018)	-0.053*** (0.018)	-0.038** (0.019)
CLI	0.590*** (0.109)	0.587*** (0.130)	0.425*** (0.134)	0.305** (0.135)	0.159 (0.138)
Adj. R^2	0.351	0.105	0.066	0.080	0.074
Obs	243	241	238	235	232

Notes: This table presents the results of the predictive regressions between the industry uncertainty network connectedness, and the coincident indicators of business cycle, namely CFNAI and ADS. We present results for regression equation 9 in which we add a set of controls including also the leading indicator, CLI. The five columns of the table represent different predictability horizons with $h \in (1, 3, 6, 9, 12)$. Regressions' coefficients and standard errors (in parentheses), and adjusted- R^2 are reported. Coefficients are marked with *, **, *** for 10%, 5%, 1% significance levels, respectively. Intercept and controls results are not reported for the sake of space, the only exception being the CLI control. Series are considered at monthly frequency between 01-2000 and 05-2020.

We show how the uncertainty network predictability holds at every horizon, even after controlling for CLI. The latter shows a good predictive ability, however up to the 9-month horizon, in line with the index characteristics description. The uncertainty network clearly shows evidence of a complementary and rather superior business cycles leading indicator spanning predictive power from 1- to 12-month horizon in advance, even after controlling for CLI. For the ADS, as a proxy for a coincident business cycle indicator, we find a weaker

predictive power for the uncertainty network at the short horizon, however still confirming the anticipatory property of about one quarter.

Finally, we repeat the same exercise of Table 5 by adopting the USLI indicator by the ECRI as control. We obtain similar findings for both CFNAI and ADS and results are relegated to the paper appendix in Table F3. Overall, the uncertainty network adds quite a lot in terms of long horizon predictability compared to the information content of other leading indicators of business cycles.

6.3 Predicting the volatility of GDP

Finally, inspired by [Carvalho and Gabaix \(2013\)](#), in this section we check whether or not our uncertainty network connectedness is also able to predict future US GDP growth rate and volatility. We calculate the growth rate of GDP_t , the US GDP at time t as $g_t = \log(GDP_{t+1}/GDP_t)$ where t is expressed in quarterly frequency.²⁹ The volatility of GDP growth is measured as the annualized GDP standard deviation over 4 quarters. We check whether or not the aggregate network is able to predict US GDP indicators in the next h quarters ahead, with $h \in (1, 2, 3, 4)$ by running the predictive equation 9 at quarterly frequency.

We report the empirical results in Table F1 in appendix. We observe that the uncertainty network is able to predict future GDP growth rate at 2 and 3 quarters ahead. An intensification of connections leads to a decreasing GDP growth rate in the following quarters. We then show how the information enclosed in our measures is also useful to predict future GDP volatility. By repeating the same exercise, we also show that network is able to predict future GDP volatility in the next four quarters, the results being even stronger and found to be significant up to one year. An increase in connectedness leads to an increase in GDP volatility, thus confirming the counter-cyclicality of uncertainty network.

²⁹In [Carvalho and Gabaix \(2013\)](#) the model for volatility is annual, while we are aggregating our series to a quarterly frequency, end of the quarter.

6.4 Hubs and non-hubs industry connectedness networks

In this subsection we check whether the predictability power of uncertainty hubs-based networks may differ from the one of uncertainty non-hubs. We repeat the empirical analysis of the previous section, now considering only hubs and non-hubs based networks, $\mathcal{C}_t^{\text{hub}}$ and $\mathcal{C}_t^{\text{non-hub}}$, respectively. We hypothesize that the former leads to a greater predictability since reflecting information from the industries detected to be the main uncertainty contributors within the system. For the main empirical analysis both networks are constructed with CD, CM, E, IN and IT industries included in the dynamic uncertainty hubs network, and F, M, RE and U industries in the uncertainty non-hubs network.³⁰ Similarly to equation 9, we estimate the following:

$$\mathcal{Y}_{t+h}^{(\ell)} = \beta_0 + \beta_{\text{hub}} \mathcal{C}_t^{\text{hub}} + \beta_{\text{non-hub}} \mathcal{C}_t^{\text{non-hub}} + \sum_{i=1}^N \beta_{X,i} X_{t,i} + \epsilon_t \quad (10)$$

where we add the independent variables that characterize uncertainty hubs and non-hubs based on network connectedness taken jointly and aggregated at monthly frequency in order to match the frequency of the indicators we adopt. We include the same set of controls X .

In Table 6 we observe that the predictability of the hubs network is superior compared to the non-hubs with respect to the aggregate CFNAI-MA3 and recessions especially for longer horizons, while with respect to expansion at any horizons. We notice how the result achieved by looking at the predictive ability of uncertainty network resemble, or appear even stronger than, the results obtained in the previous section when looking at the aggregated predictability.³¹ This shows how the aggregated network connectedness results might be actually driven by few industry uncertainty hubs, these achieving predictability with respect to business cycles which is at times even stronger than the entire aggregated industry network.

³⁰See also Table 2 and Figure 3.

³¹In Table F1 in the appendix we show the results of the $\mathcal{C}^{(H)}$ predictor alone with controlling for X which leads to a similar conclusion and findings similar to the aggregate network \mathcal{C} as well. $\mathcal{C}^{(H)}$ is found to be able to predict well the business cycle up to one year in advance. The more focused number of uncertainty hubs network $\mathcal{C}^{(H)}$ confirms the strong predictive ability also with respect to expansion and recession periods.

Table 6: Hubs vs no-Hubs Network Predictive Results

Panel A: CFNAI-MA3					
	$h=1$	$h=3$	$h=6$	$h=9$	$h=12$
$\mathcal{C}_t^{\text{hub}} X_t$	-0.007* (0.004)	-0.013*** (0.004)	-0.017*** (0.004)	-0.021*** (0.004)	-0.019*** (0.004)
$\mathcal{C}_t^{\text{non-hub}} X_t$	-0.015*** (0.006)	-0.021*** (0.006)	-0.013* (0.007)	-0.010 (0.007)	0.002 (0.007)
Adj. R^2	0.319	0.214	0.115	0.183	0.183
Obs	243	241	238	235	232
Panel B: CFNAI-MA3 Expansion					
	$h=1$	$h=3$	$h=6$	$h=9$	$h=12$
$\mathcal{C}_t^{\text{hub}} X_t$	-0.004*** (0.001)	-0.005*** (0.001)	-0.005*** (0.001)	-0.006*** (0.001)	-0.006*** (0.001)
$\mathcal{C}_t^{\text{non-hub}} X_t$	0.001 (0.002)	-0.001 (0.002)	-0.005*** (0.002)	-0.001 (0.002)	0.0004 (0.002)
Adj. R^2	0.097	0.150	0.258	0.289	0.286
Obs	243	241	238	235	232
Panel C: CFNAI-MA3 Recession					
	$h=1$	$h=3$	$h=6$	$h=9$	$h=12$
$\mathcal{C}_t^{\text{hub}} X_t$	-0.003 (0.004)	-0.008** (0.004)	-0.012*** (0.004)	-0.015*** (0.004)	-0.012*** (0.004)
$\mathcal{C}_t^{\text{non-hub}} X_t$	-0.016*** (0.005)	-0.020*** (0.006)	-0.009 (0.007)	-0.009 (0.006)	0.002 (0.006)
Adj. R^2	0.313	0.190	0.090	0.152	0.149
Obs	243	241	238	235	232

Notes: This table presents the results of the predictive regression 10 comparing the predictive ability of the uncertainty hubs vs non-hubs sub-networks with respect to the 3-month moving average of the Chicago FED National Activity Index (CFNAI-MA3) in Panel A. In Panel B and Panel C the results of the predictive regression with respect to the CFNAI expansion and recession periods are reported, respectively. The five columns of the table represent different predictability horizons with $h \in (1, 3, 6, 9, 12)$. Regressions' coefficients and standard errors (in parentheses), and adjusted- R^2 are reported. Coefficients are marked with *, **, *** for 10%, 5%, 1% significance levels, respectively. Intercept and controls results are not reported for the sake of space, the only exception being the CLI control. Series are considered at monthly frequency between 01-2000 and 05-2020.

We then check the relationship between the hubs and non-hubs networks with respect to leading indicators of the business cycle. The predictive results with respect to CLI are reported in Table 7. We find that hubs network connectedness is able to strongly predict the leading indicator of business cycle up to one year, whereas the predictive power of non-hubs network is overall absent. Thus, uncertainty hubs show strong predictive power with respect to coincident measures of the business cycle, however this being even stronger with respect to leading indicators of business cycle, confirming a clear superior ability in predicting these indicators compared to non-hubs.

As in the previous section, now we validate the predictive ability of the hubs based

network by including the leading indicator CLI to the multivariate regression when predicting CFNAI-MA3 as a control variable. The hubs network shows strong predictive ability from 3-month up to one year being the most timely indicator of the business cycle since it is able to predict coincident indicators one-year in advance. The non-hub network shows good predictive power in the short horizon. On the other hand, the hubs network is found to complement the shorter horizon predictive ability of CLI, expanding it to longer horizons. Therefore while the predictive ability of the hubs network connectedness spans over longer horizons, up to one year, the predictive ability of non-hubs is found to be limited to shorter horizons up to 6 months, therefore it appears not to contain additional information compared to other leading indicators of business cycles e.g. CLI. The hubs-based network shows a longer horizon predictive power, useful feature for any leading indicators of business cycle. This further echoes the results obtained with the aggregate uncertainty network, therefore we can conclude that the hubs-based network may be considered as the main driver of the aggregate network, achieving even stronger predictive power on its own.

As a robustness check, we also repeat the same predictive exercises by adopting a stricter construction of the hubs and non-hubs networks, including only CM, IN and IT industries and M, RE and U in the networks respectively. We report the results in Table F2 in appendix with respect to all the coincident indicator CFNAI-MA3, expansions and recessions, and also with respect to the leading indicator CLI. We corroborates our previous findings and confirm our hypothesis since the hubs network is found to be more informative in predicting well the future business cycle indicators. The new non-hubs however shows better predictability with respect to the aggregate CFNAI-MA3 and recessions.

Finally, we also study the predictive ability of hubs and non-hubs based uncertainty networks with respect to GDP growth rate and volatility as show the results in Table F3 in appendix. Also, in this case, we find a stronger predictive ability for the hubs network compared to non-hubs with respect to both GDP growth rate and GDP volatility. We confirm the asymmetric predictive ability of the uncertainty network in favour of the hubs

Table 7: Hubs vs no-Hubs Network Predictive Results

Panel A: Leading Indicator CLI					
	$h=1$	$h=3$	$h=6$	$h=9$	$h=12$
$\mathcal{C}_t^{\text{hub}} X_t$	-0.012** (0.005)	-0.024*** (0.006)	-0.039*** (0.006)	-0.051*** (0.006)	-0.056*** (0.006)
$\mathcal{C}_t^{\text{non-hub}} X_t$	-0.009 (0.008)	-0.015 (0.009)	-0.016 (0.010)	-0.017* (0.010)	-0.005 (0.010)
Adj. R^2	0.447	0.335	0.269	0.325	0.339
Obs	243	241	238	235	232
Panel B: CFNAI-MA3 controlling for CLI					
	$h=1$	$h=3$	$h=6$	$h=9$	$h=12$
$\mathcal{C}_t^{\text{hub}} X_t$	-0.003 (0.003)	-0.009*** (0.004)	-0.015*** (0.004)	-0.020*** (0.004)	-0.019*** (0.004)
$\mathcal{C}_t^{\text{non-hub}} X_t$	-0.014*** (0.004)	-0.021*** (0.005)	-0.012* (0.007)	-0.011 (0.007)	0.002 (0.007)
CLI	0.424*** (0.036)	0.340*** (0.044)	0.243*** (0.051)	0.109** (0.051)	-0.017 (0.053)
Adj. R^2	0.573	0.371	0.193	0.196	0.179
Obs	243	241	238	235	232

Notes: This table presents the results of the predictive regression 10 comparing the predictive ability of the uncertainty hubs vs non-hubs sub-networks with respect to the leading indicator, CLI (Panel A). In Panel B, the results with respect to the CFNAI-MA3 coincident indicator controlling also for the leading indicator, CLI, are reported. The five columns of the table represent different predictability horizons with $h \in (1, 3, 6, 9, 12)$. Regressions' coefficients and standard errors (in parentheses), and adjusted- R^2 are reported. Coefficients are marked with *, **, *** for 10%, 5%, 1% significance levels, respectively. Intercept and controls results are not reported for the sake of space, the only exception being the CLI control. Series are considered at monthly frequency between 01-2000 and 05-2020.

network, while weak and almost absent predictive power for non-hubs network. We also confirm stronger results for the hubs network compared to the aggregate network results of the previous subsection, emphasizing once more how a network extracted solely from uncertainty hubs might have even strong predictive power not only with respect to the indicators of the business cycle, but also with respect to the volatility of GDP.

7 Conclusion

We studied the ex ante uncertainty network of the US industries constructed from options-based investors future expectations about one month ahead uncertainty. We relied on a novel data set of industry forward looking uncertainties and we adopted a time varying parameter VAR (TVP-VAR) to model the ex-ante uncertainty network of industries.

We were able to obtain a precise point in time estimation of the uncertainty network to

accurately characterize the specific industry role in shocks to uncertainty, dynamically over the business cycle. We uncovered a main role for booming industries such as communications and information technology and we classified these as uncertainty hubs. Industries such as, financial (important role mainly limited to the global financial crisis), real estate, materials and utilities showed a more neutral role and are classified as uncertainty non-hubs.

Our industry uncertainty network is also forward-looking since constructed from options. We exploited the forward-looking industry connectedness networks characteristics in predictability. We found the industry uncertainty network to be a useful tool to predict future business cycles. We also showed that networks extracted from uncertainty hubs are the main drivers of the predictive power of the aggregate network.

We provided new insights about time-varying interactions between the newly constructed ex ante industry uncertainty network for the US and the business cycles. The uncertainty network may serve as new tool for regulators and policy makers in order to monitor the relationship between industry networks, the business cycle, e.g. recessions and expansions, and the real economy, in a precise, timely and forward-looking manner. More focus should be placed on uncertainty hubs since they are the stronger contributors to uncertainty shocks and the main predictors of the real economy. This implies that fluctuations in uncertainty with respect to uncertainty hubs should be more carefully monitored due to its potential for shaping the US industry networks and impacting the real economy.

References

- Acemoglu, D. and P. D. Azar (2020). Endogenous production networks. *Econometrica* 88(1), 33–82.
- Acemoglu, D., V. M. Carvalho, A. Ozdaglar, and A. Tahbaz-Salehi (2012). The network origins of aggregate fluctuations. *Econometrica* 80(5), 1977–2016.
- Acemoglu, D., A. Ozdaglar, and A. Tahbaz-Salehi (2017). Microeconomic origins of macroeconomic tail risks. *American Economic Review* 107(1), 54–108.
- Adrian, T. and A. Estrella (2008). Monetary tightening cycles and the predictability of economic activity. *Economics Letters* 99(2), 260–264.
- Arellano, C., Y. Bai, and P. J. Kehoe (2019). Financial frictions and fluctuations in volatility. *Journal of Political Economy* 127(5), 2049–2103.
- Atalay, E. (2017). How important are sectoral shocks? *American Economic Journal: Macroeconomics* 9(4), 254–80.
- Auer, R. A., A. A. Levchenko, and P. Sauré (2019). International inflation spillovers through input linkages. *Review of Economics and Statistics* 101(3), 507–521.
- Bachmann, R. and C. Bayer (2014). Investment dispersion and the business cycle. *American Economic Review* 104(4), 1392–1416.
- Bachmann, R., S. Elstner, and E. R. Sims (2013). Uncertainty and economic activity: Evidence from business survey data. *American Economic Journal: Macroeconomics* 5(2), 217–49.
- Bakshi, G., N. Kapadia, and D. Madan (2003). Stock return characteristics, skew laws, and the differential pricing of individual equity options. *Review of Financial Studies* 16(1), 101–143.
- Bakshi, G. and D. Madan (2000). Spanning and derivative-security valuation. *Journal of Financial Economics* 55(2), 205–238.
- Baqaei, D. R. and E. Farhi (2019). The macroeconomic impact of microeconomic shocks: beyond Hulten’s theorem. *Econometrica* 87(4), 1155–1203.
- Barrot, J.-N. and J. Sauvagnat (2016). Input specificity and the propagation of idiosyncratic shocks in production networks. *The Quarterly Journal of Economics* 131(3), 1543–1592.
- Baruník, J., M. Bevilacqua, and R. Tunaru (2020). Asymmetric network connectedness of fears. *The Review of Economics and Statistics* forthcoming.
- Barunik, J. and M. Ellington (2020). Dynamic networks in large financial and economic systems. *arXiv preprint arXiv:2007.07842*.

- Berge, T. J. and Ò. Jordà (2011). Evaluating the classification of economic activity into recessions and expansions. *American Economic Journal: Macroeconomics* 3(2), 246–77.
- Bloom, N. (2009). The impact of uncertainty shocks. *Econometrica* 77(3), 623–685.
- Bloom, N. (2014). Fluctuations in uncertainty. *Journal of Economic Perspectives* 28(2), 153–76.
- Bloom, N., M. Floetotto, N. Jaimovich, I. Saporta-Eksten, and S. J. Terry (2018). Really uncertain business cycles. *Econometrica* 86(3), 1031–1065.
- Carr, P. and R. Lee (2009). Volatility derivatives. *Annu. Rev. Financ. Econ.* 1(1), 319–339.
- Carr, P. and L. Wu (2006). A tale of two indices. *The Journal of Derivatives* 13(3), 13–29.
- Carrieri, F., V. Errunza, and S. Sarkissian (2004). Industry risk and market integration. *Management Science* 50(2), 207–221.
- Carvalho, V. and X. Gabaix (2013). The great diversification and its undoing. *American Economic Review* 103(5), 1697–1727.
- Carvalho, V. M. and A. Tahbaz-Salehi (2019). Production networks: A primer. *Annual Review of Economics* 11, 635–663.
- Cheng, I.-H. (2019). The VIX premium. *The Review of Financial Studies* 32(1), 180–227.
- Christensen, B. J. and N. R. Prabhala (1998). The relation between implied and realized volatility. *Journal of Financial Economics* 50(2), 125–150.
- Christiano, L. J., R. Motto, and M. Rostagno (2014). Risk shocks. *American Economic Review* 104(1), 27–65.
- Dahlhaus, R. (1996). On the Kullback-Leibler information divergence of locally stationary processes. *Stochastic Processes and their Applications* 62(1), 139–168.
- Dahlhaus, R., W. Polonik, et al. (2009). Empirical spectral processes for locally stationary time series. *Bernoulli* 15(1), 1–39.
- Decker, R. A., P. N. D’Erasmus, and H. Moscoso Boedo (2016). Market exposure and endogenous firm volatility over the business cycle. *American Economic Journal: Macroeconomics* 8(1), 148–98.
- Di Giovanni, J., A. A. Levchenko, and I. Mejean (2014). Firms, destinations, and aggregate fluctuations. *Econometrica* 82(4), 1303–1340.
- Diebold, F. X. and K. Yilmaz (2012). Better to give than to receive: Predictive directional measurement of volatility spillovers. *International Journal of Forecasting* 28(1), 57–66.
- Diebold, F. X. and K. Yilmaz (2014). On the network topology of variance decompositions: Measuring the connectedness of financial firms. *Journal of Econometrics* 182(1), 119–134.

- Filipović, D., E. Gourié, and L. Mancini (2016). Quadratic variance swap models. *Journal of Financial Economics* 119(1), 44–68.
- Gabaix, X. (2011). The granular origins of aggregate fluctuations. *Econometrica* 79(3), 733–772.
- Gabaix, X. (2016). Power laws in economics: An introduction. *Journal of Economic Perspectives* 30(1), 185–206.
- Griffin, J. M., X. Ji, and J. S. Martin (2003). Momentum investing and business cycle risk: Evidence from pole to pole. *The Journal of Finance* 58(6), 2515–2547.
- Griffin, J. M. and G. A. Karolyi (1998). Another look at the role of the industrial structure of markets for international diversification strategies. *Journal of Financial Economics* 50(3), 351–373.
- Griffin, J. M. and R. M. Stulz (2001). International competition and exchange rate shocks: a cross-country industry analysis of stock returns. *The Review of Financial Studies* 14(1), 215–241.
- Herskovic, B., B. T. Kelly, H. N. Lustig, and S. Van Nieuwerburgh (2020). Firm volatility in granular networks. *Journal of Political Economy* (12-56).
- Jurado, K., S. C. Ludvigson, and S. Ng (2015). Measuring uncertainty. *American Economic Review* 105(3), 1177–1216.
- Kadiyala, K. R. and S. Karlsson (1997). Numerical methods for estimation and inference in Bayesian VAR-models. *Journal of Applied Econometrics* 12(2), 99–132.
- Lehn, C. v. and T. Winberry (2020). The investment network, sectoral comovement, and the changing US business cycle. Technical report.
- Ludvigson, S., S. Ma, and S. Ng (2020). Uncertainty and business cycles: Exogenous impulse or endogenous response? *American Economic Journal: Macroeconomics*.
- Ozdagli, A. and M. Weber (2017). Monetary policy through production networks: Evidence from the stock market. *National Bureau of Economic Research Working Paper*.
- Pástor, L. and P. Veronesi (2009). Technological revolutions and stock prices. *American Economic Review* 99(4), 1451–83.
- Pesaran, H. H. and Y. Shin (1998). Generalized impulse response analysis in linear multivariate models. *Economics letters* 58(1), 17–29.
- Petrova, K. (2019). A quasi-Bayesian local likelihood approach to time varying parameter VAR models. *Journal of Econometrics*.
- Rambachan, A. and N. Shephard (2019). Econometric analysis of potential outcomes time series: instruments, shocks, linearity and the causal response function. *arXiv preprint arXiv:1903.01637*.

- Roueff, F. and A. Sanchez-Perez (2016). Prediction of weakly locally stationary processes by auto-regression. *arXiv preprint arXiv:1602.01942*.
- Santa-Clara, P. and S. Yan (2010). Crashes, volatility, and the equity premium: Lessons from S&P 500 options. *Review of Economics and Statistics* 92(2), 435–451.

Appendix

Appendix A S&P 500 sectors breakdown

In this short section we present a U.S. stock market sectors breakdown and description where the S&P 500 index is used as a proxy for the stock market. The information in this section are reported as of January 25, 2019. For more details and updated information, see also <https://us.spindices.com/indices/equity/sp-500>.

- **Consumer Discretionary:** The consumer discretionary sector consists of businesses that have demand that rises and falls based on general economic conditions such as washers and dryers, sporting goods, new cars, and diamond engagement rings. At present, the consumer discretionary sector contains 11 sub-industries: Automobile Components Industry, Automobiles Industry, Distributors Industry, Diversified Consumer Services Industry, Hotels, Restaurants & Leisure Industry, Household Durables Industry, Leisure Products Industry, Multiline Retail Industry, Specialty Retail Industry, Textile, Apparel & Luxury Goods Industry, Internet & Direct Marketing. The total value of all consumer discretionary stocks in the United States came to \$4.54 trillion, or about 10.11% of the market. Examples of consumer discretionary stocks include Amazon and Starbucks.
- **Communication Services:** From telephone access to high-speed internet, the communication services sector of the economy keeps us all connected. At present, the communication services sector is made up of five industries: Diversified Telecommunication Services, Wireless Telecommunication Services, Entertainment Media, Interactive Media and Services. the total value of all communication services stocks in the United States came to \$4.42 trillion, or 10.33% of the market. The communications industry includes stocks such as AT&T and Verizon, but also the giants Alphabet Inc A and Facebook from 2004 and 2012, respectively.
- **Consumer Staples:** The consumer staples sector consists of businesses that sell the necessities of life, ranging from bleach and laundry detergent to toothpaste and packaged food. At present, the consumer staples sector contains six industries: Beverages Industry, Food & Staples Retailing Industry, Food Products Industry, Household Products Industry, Personal Products Industry, Tobacco Industry. The total value of all consumer staples stocks in the United States came to \$2.95 trillion, or about 7.18% of the market and includes companies such as Procter & Gamble.
- **Energy:** The energy sector consists of businesses that source, drill, extract, and refine the raw commodities we need to keep the country going, such as oil and gas. At present, the energy sector contains two industries: Energy Equipment & Services Industry, and Oil, Gas & Consumable Fuels Industry. The total value of all energy stocks in the United States came to \$3.36 trillion, or about 5.51% of the market. Major energy stocks include Exxon Mobil and Chevron.
- **Financial:** The financial sector consists of banks, insurance companies, real estate investment trusts, credit card issuers. At present, the financial sector contains seven

industries: Banking Industry, Capital Markets Industry, Consumer Finance Industry, Diversified Financial Services Industry, Insurance Industry, Mortgage Real Estate Investment Trusts (REITs) Industry, Thrifts & Mortgage Finance Industry. The total value of all financial stocks in the United States came to \$6.89 trillion, or about 13.63% of the market. JPMorganChase, GoldmanSachs, and Bank of America are examples of financial stocks.

- Health Care: The health care sector consists of drug companies, medical supply companies, and other scientific-based operations that are concerned with improving and healing human life. At present, the health care sector contains six industries: Biotechnology Industry, Health Care Equipment & Supplies Industry, Health Care Providers & Services Industry, Health Care Technology Industry, Life Sciences Tools & Services Industry, Pharmaceuticals Industry. The total value of all health care stocks in the United States came to \$5.25 trillion, or about 15.21% of the market. Examples of health care stocks include Johnson & Johnson, and Pfizer.
- Industrials: The industrial sector comprises railroads and airlines to military weapons and industrial conglomerates. At present, the industrial sector contains fourteen industries: Aerospace & Defense Industry, Air Freight & Logistics Industry, Airlines Industry, Building Products Industry, Commercial Services & Supplies Industry, Construction & Engineering Industry, Electrical Equipment Industry, Industrial Conglomerates Industry, Machinery Industry, Marine Industry, Professional Services Industry, Road & Rail Industry, Trading Companies & Distributors Industry, Transportation Infrastructure Industry. The total value of all industrial stocks in the United States came to \$3.80 trillion, or about 9.33% of the market.
- Information Technology: the information technology (IT) sector is home to the hardware, software, computer equipment, and IT services operations that make it possible for you to be reading this right now. At present, the information technology sector contains six industries: Communications Equipment Industry, Electronic Equipment, Instruments & Components Industry, IT Services Industry, Semiconductors & Semiconductor Equipment Industry, Software Industry, Technology Hardware, Storage & Peripherals Industry. The total value of all information technology stocks in the United States came to \$7.10 trillion, or about 19.85% of the market. It is the largest sector in the S&P 500. Top IT stocks include Microsoft and Apple.
- Materials: The building blocks that supply the other sectors with the raw materials it needs to conduct business, the material sector manufacturers, logs, and mines everything from precious metals, paper, and chemicals to shipping containers, wood pulp, and industrial ore. At present, the material sector contains five industries: Chemicals Industry, Construction Materials Industry, Containers & Packaging Industry, Metals & Mining Industry, Paper & Forest Products Industry. The total value of all materials stocks in the United States came to \$1.77 trillion, or about 2.71% of the market. Major materials stocks include Dupont.
- Real Estate: The real estate sector includes all Real Estate Investment Trusts (REITs) with the exception of Mortgage REITs, which is housed under the financial sector. The

sector also includes companies that manage and develop properties. At present, the Real Estate sector is made up of two industries: Equity Real Estate Investment Trusts, Real Estate Management & Development. The total value of all real estate stocks in the United States came to \$1.17 trillion, or 2.96% of the market. The real estate industry includes stocks such as Simon Property Group and Prologis.

- Utilities: The utilities sector of the economy is home to the firms that make our lights work when we flip the switch, let our stoves erupt in flame when we want to cook food, make water come out of the tap when we are thirsty, and more. At present, the utilities sector is made up of five industries: Electric Utilities Industry, Gas Utilities Industry, Independent Power and Renewable Electricity Producers Industry, Multi-Utilities Industry, Water Utilities Industry. The total value of all utilities stocks in the United States came to \$1.27 trillion, or about 3.18% of the market. Utilities stocks include many local electricity and water companies including Dominion Resources.

Appendix B Model-free individual implied volatility

Formalizing the implied volatility computation for each stock, we follow [Bakshi et al. \(2003\)](#) in adopting out-of-the-money (OTM) call and put option prices to compute the individual stock s th implied variance as

$$\sigma_{\text{VIX}(s)}^2 = \int_{P_t}^{\infty} \frac{2(1 - \log(K/P_t))}{K^2} C(t, t+1, K) dK + \int_0^{P_t} \frac{2(1 + \log(P_t/K))}{K^2} P(t, t+1, K) dK, \quad (11)$$

where $C(\cdot)$ and $P(\cdot)$ denote the time t prices of call and put contracts, respectively, with time to maturity of one period and a strike price of K .

Intuitively, the implied variance measure can be computed in a model-free way from a range of option prices upon a discretization of formula (11), adopting call and put option prices with respect to the next 30 days, considering all available strikes for each individual stock options. We compute the $\text{VIX}^{(s)}$ for all the stocks in our sample belonging to the 11 US industries as follows:

$$\sigma_{\text{VIX}(s)}^2 = \frac{2}{T} \sum_{i=1}^n \frac{\Delta K_i}{K_i^2} e^{rT} Q(K_i) - \frac{1}{T} \left[\frac{F}{K_0} - 1 \right]^2, \quad (12)$$

where T is time to expiration, F is the forward index level derived from the put-call parity as $F = e^{rT}[C(K, T) - P(K, T)] + K$ with the risk-free rate r , K_0 is the reference price, the first exercise price less or equal to the forward level F ($K_0 \leq F$), and K_i is the i th out-of-the-money (OTM) strike price available on a specific date (call if $K_i > K_0$, put if $K_i < K_0$, and both call and put if $K_i = K_0$). $Q(K_i)$ is the average bid-ask of OTM options with exercise price equal to K_i . If $K_i = K_0$, it will be equal to the average between the at-the-money (ATM) call and put price, relative to the strike price, and $\Delta(K_i)$ is the sum divided by two of the two nearest prices to the exercise price K_0 , namely, $\frac{(K_{i+1} - K_{i-1})}{2}$ for $2 \leq i \leq n-1$. The annualized square roots of the quantities computed for each of the s -th individual companies are then labeled $\text{VIX}^{(s)}$ denoting individual, model-free implied volatility measures of the expected price fluctuations in the s -th underlying asset's options over the next month.³²

$$\text{VIX}^{(s)} = \sqrt{\frac{365}{30} \sigma_{\text{VIX}(s)}^2} \quad (13)$$

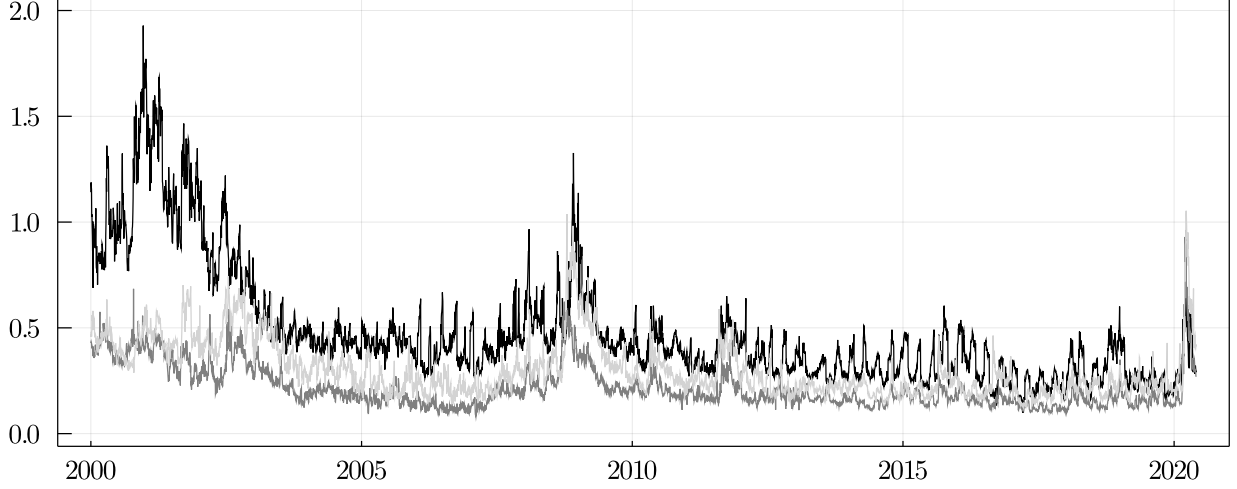
³²The standard CBOE methodology considers an interpolation between the two closest to 30-days expiration dates. We use a simplified formula taking into account only one expiration date closest to 30-days due to options data availability with respect to US single stocks.

Table A1: List of Selected Stocks by Industry

Ticker	Full name	Period	Ticker	Full name	Period
Consumer discretionary:			Industrial		
AMZN	Amazon.com Inc.	1996-2020	BA	Boeing Company	1996-2020
HD	Home Depot Inc.	1996-2020	GE	General Electric Company	1996-2020
MCD	McDonald's Corporation	1996-2020	HON	Honeywell International Inc.	1996-2020
NKE	NIKE Inc. Class B	1996-2020	UNP	Union Pacific Corporation	1996-2020
SBUX	Starbucks Corporation	1996-2020	UTX	United Technologies Corporation	1996-2018
			CAT	Caterpillar Inc.	2019-2020
Communications:			Information Technology		
CMCSA	Comcast Corporation Class A	1996-2004	AAPL	Apple Inc.	1996-2020
DIS	Walt Disney Company	1996-2020	ADBE	Adobe Inc.	1996-2020
EA	Electronic Arts Inc.	1996-2015	CSCO	Cisco Systems Inc.	1996-2015
FB	Facebook Inc. Class A	2012-2020	INTC	Intel Corporation	1996-2020
GOOG	Alphabet Inc. Class C	2004-2020	MA	Mastercard Incorporated Class A	2007-2018
T	AT&T Inc.	1996-2020	MSFT	Microsoft Corporation	1996-2020
VZ	Verizon Communications Inc.	1996-2020	V	Visa Inc. Class A	2008-2020
Consumer staples:			Materials		
COST	Costco Wholesale Corporation	1996-2018	APD	Air Products and Chemicals Inc	1996-2018
KO	Coca-Cola Company	1996-2020	DD	DuPont de Nemours Inc.	1996-2018
PEP	PepsiCo Inc.	1996-2020	ECL	Ecolab Inc.	1996-2018
PG	Procter & Gamble Company	1996-2020	LIN	Linde plc	1996-2007
WMT	Walmart Inc.	1996-2020	PPG	PPG Industries Inc.	2007-2018
PM	Philip Morris Inc.	2018-2020	SHW	Sherwin-Williams Company	1998-2020
			NEM	Newmont Corporation	2019-2020
			FCX	Freeport-McMoRan Inc.	2019-2020
			IP	International Paper	2019-2020
Energy:			Real Estate		
COP	ConocoPhillips	1996-2020	AMT	American Tower Corporation	1996-2020
CVX	Chevron Corporation	1996-2020	CCI	Crown Castle International Corp	1996-2018
SLB	Schlumberger NV	1996-2020	EQIX	Equinix Inc.	2006-2020
XOM	Exxon Mobil Corporation	1996-2020	EQR	Equity Residential	1996-2020
VLO	Valero Energy Corp	1996-2015	PLD	Prologis Inc.	1996-2018
PSX	Phillips 66	2012-2020	SPG	Simon Property Group Inc.	1996-2020
Financial			Utilities		
BAC	Bank of America Corp	1996-2020	AEP	American Electric Power Company Inc.	1996-2020
BRK	Berkshire Hathaway Inc. Class B	2010-2020	D	Dominion Energy Inc	1996-2020
C	Citigroup Inc.	1996-2020	DUK	Duke Energy Corporation	2006-2020
GS	Goldman Sachs	1999-2018	NEE	NextEra Energy Inc.	1996-2020
JPM	JPMorgan Chase & Co.	1996-2020	SO	Southern Company	1996-2020
WFC	Wells Fargo & Company	1996-2020			
Health care:					
ABT	Abbott Laboratories	1996-2019			
JNJ	Johnson & Johnson	1996-2020			
MRK	Merck & Co. Inc.	1996-2020			
PFE	Pfizer Inc.	1996-2020			
UNH	UnitedHealth Group Incorporated	1996-2020			
ABBV	AbbVie Inc.	2018-2020			

Notes: This table summarizes all the US stocks selected in the paper, divided by industry. The stock tickers, full names and period of options data availability are reported.

Figure A1: **Individual Company Uncertainty**



Notes: This figure illustrates the individual uncertainty $VIX^{(i)}$ for Amazon (in black), Coca-Cola (in grey) and Disney (in light grey) from 03-01-2000 to 29-05-2020, at a daily frequency.

Appendix C Proofs

Proposition 1. Let us have the $VMA(\infty)$ representation of the locally stationary TVP VAR model (Dahlhaus et al., 2009; Roueff and Sanchez-Perez, 2016)

$$\mathbf{IVIX}_{t,T} = \sum_{h=-\infty}^{\infty} \Psi_{t,T,h} \epsilon_{t-h} \quad (14)$$

$\Psi_{t,T,h} \approx \Psi(t/T, h)$ is a stochastic process satisfying $\sup_{\ell} \|\Psi_t - \Psi_{\ell}\|^2 = O_p(h/t)$ for $1 \leq h \leq t$ as $t \rightarrow \infty$, hence in a neighborhood of a fixed time point $u = t/T$ the process $\mathbf{IVIX}_{t,T}$ can be approximated by a stationary process $\widetilde{\mathbf{IVIX}}_t(u)$

$$\widetilde{\mathbf{IVIX}}_t(u) = \sum_{h=-\infty}^{\infty} \Psi_h(u) \epsilon_{t-h} \quad (15)$$

with ϵ being *iid* process with $\mathbb{E}[\epsilon_t] = 0$, $\mathbb{E}[\epsilon_s \epsilon_t] = 0$ for all $s \neq t$, and the local covariance matrix of the errors $\Sigma(u)$. Under suitable regularity conditions $|\mathbf{IVIX}_{t,T} - \widetilde{\mathbf{IVIX}}_t(u)| = O_p(|t/T - u| + 1/T)$.

Since the errors are assumed to be serially uncorrelated, the total local covariance matrix of the forecast error conditional on the information at time $t - 1$ is given by

$$\Omega^H(u) = \sum_{h=0}^H \Psi_h(u) \Sigma(u) \Psi_h^{\top}(u). \quad (16)$$

Next, we consider the local covariance matrix of the forecast error conditional on knowledge of today's shock and future expected shocks to k -th variable. Starting from the conditional forecasting error,

$$\boldsymbol{\xi}^{k,H}(u) = \sum_{h=0}^H \boldsymbol{\Psi}_h(u) \left[\boldsymbol{\epsilon}_{t+H-h} - \mathbb{E}(\boldsymbol{\epsilon}_{t+H-h} | \boldsymbol{\epsilon}_{k,t+H-h}) \right], \quad (17)$$

assuming normal distribution of $\boldsymbol{\epsilon}_t \sim N(0, \boldsymbol{\Sigma})$, we obtain³³

$$\mathbb{E}(\boldsymbol{\epsilon}_{t+H-h} | \boldsymbol{\epsilon}_{k,t+H-h}) = \sigma_{kk}^{-1} \left[\boldsymbol{\Sigma}(u) \right]_{\cdot k} \boldsymbol{\epsilon}_{k,t+H-h} \quad (18)$$

and substituting (18) to (17), we obtain

$$\boldsymbol{\xi}^{k,H}(u) = \sum_{h=0}^H \boldsymbol{\Psi}_h(u) \left[\boldsymbol{\epsilon}_{t+H-h} - \sigma_{kk}^{-1} \left[\boldsymbol{\Sigma}(u) \right]_{\cdot k} \boldsymbol{\epsilon}_{k,t+H-h} \right]. \quad (19)$$

Finally, the local forecast error covariance matrix is

$$\boldsymbol{\Omega}^{k,H}(u) = \sum_{h=0}^H \boldsymbol{\Psi}_h(u) \boldsymbol{\Sigma}(u) \boldsymbol{\Psi}_h^\top(u) - \sigma_{kk}^{-1} \sum_{h=0}^H \boldsymbol{\Psi}_h(u) \left[\boldsymbol{\Sigma}(u) \right]_{\cdot k} \left[\boldsymbol{\Sigma}(u) \right]_{\cdot k}^\top \boldsymbol{\Psi}_h^\top(u). \quad (20)$$

Then

$$\left[\boldsymbol{\Delta}^H(u) \right]_{(j)k} = \left[\boldsymbol{\Omega}^H(u) - \boldsymbol{\Omega}^{k,H}(u) \right]_{j,j} = \sigma_{kk}^{-1} \sum_{h=0}^H \left(\left[\boldsymbol{\Psi}_h(u) \boldsymbol{\Sigma}(u) \right]_{j,k} \right)^2 \quad (21)$$

is the unscaled local H -step ahead forecast error variance of the j -th component with respect to the innovation in the k -th component. Scaling the equation with H -step ahead forecast error variance with respect to the j th variable yields the desired time varying generalized forecast error variance decompositions (TVP GFEVD)

$$\left[\boldsymbol{\theta}^H(u) \right]_{j,k} = \frac{\sigma_{kk}^{-1} \sum_{h=0}^H \left(\left[\boldsymbol{\Psi}_h(u) \boldsymbol{\Sigma}(u) \right]_{j,k} \right)^2}{\sum_{h=0}^H \left[\boldsymbol{\Psi}_h(u) \boldsymbol{\Sigma}(u) \boldsymbol{\Psi}_h^\top(u) \right]_{j,j}} \quad (22)$$

This completes the proof. □

³³Note to notation: $[\mathbf{A}]_{j,k}$ denotes the j th row and k th column of matrix \mathbf{A} denoted in bold. $[\mathbf{A}]_{j,\cdot}$ denotes the full j th row; this is similar for the columns. A $\sum A$, where A is a matrix that denotes the sum of all elements of the matrix A .

Appendix D Estimation of the time-varying parameter VAR model

To estimate our high dimensional systems, we follow the Quasi-Bayesian Local-Likelihood (QBLL) approach of [Petrova \(2019\)](#). let \mathbf{IVIX}_t be an $N \times 1$ vector generated by a stable time-varying parameter (TVP) heteroskedastic VAR model with p lags:

$$\mathbf{IVIX}_{t,T} = \Phi_1(t/T)\mathbf{IVIX}_{t-1,T} + \dots + \Phi_p(t/T)\mathbf{IVIX}_{t-p,T} + \epsilon_{t,T}, \quad (23)$$

where $\epsilon_{t,T} = \Sigma^{-1/2}(t/T)\eta_{t,T}$ with $\eta_{t,T} \sim NID(0, \mathbf{I}_M)$ and $\Phi(t/T) = (\Phi_1(t/T), \dots, \Phi_p(t/T))^\top$ are the time varying autoregressive coefficients. Note that all roots of the polynomial, $\chi(z) = \det(\mathbf{I}_N - \sum_{p=1}^L z^p \mathbf{B}_{p,t})$, lie outside the unit circle, and Σ_t^{-1} is a positive definite time-varying covariance matrix. Stacking the time-varying intercepts and autoregressive matrices in the vector $\phi_{t,T}$ with $\overline{\mathbf{IVIX}}_t^\top = (\mathbf{I}_N \otimes x_t)$, $x_t = (1, x_{t-1}^\top, \dots, x_{t-p}^\top)$ and \otimes denotes the Kronecker product, the model can be written as:

$$\mathbf{IVIX}_{t,T} = \overline{\mathbf{IVIX}}_{t,T}^\top \phi_{t,T} + \Sigma_{t/T}^{-\frac{1}{2}} \eta_{t,T} \quad (24)$$

We obtain the time-varying parameters of the model by employing Quasi-Bayesian Local Likelihood (QBLL) methods. Estimation of (23) requires re-weighting the likelihood function. Essentially, the weighting function gives higher proportions to observations surrounding the time period whose parameter values are of interest. The local likelihood function at time period k is given by:

$$\begin{aligned} & \mathbf{L}_k(\mathbf{IVIX} | \theta_k, \Sigma_k, \overline{\mathbf{IVIX}}) \propto \\ & |\Sigma_k|^{\text{trace}(\mathbf{D}_k)/2} \exp \left\{ -\frac{1}{2} (\mathbf{IVIX} - \overline{\mathbf{IVIX}}^\top \phi_k)^\top (\Sigma_k \otimes \mathbf{D}_k) (\mathbf{IVIX} - \overline{\mathbf{IVIX}}^\top \phi_k) \right\} \end{aligned} \quad (25)$$

The \mathbf{D}_k is a diagonal matrix whose elements hold the weights:

$$\mathbf{D}_k = \text{diag}(\varrho_{k1}, \dots, \varrho_{kT}) \quad (26)$$

$$\varrho_{kt} = \phi_{T,k} w_{kt} / \sum_{t=1}^T w_{kt} \quad (27)$$

$$w_{kt} = (1/\sqrt{2\pi}) \exp((-1/2)((k-t)/H)^2), \quad \text{for } k, t \in \{1, \dots, T\} \quad (28)$$

$$\zeta_{Tk} = \left(\left(\sum_{t=1}^T w_{kt} \right)^2 \right)^{-1} \quad (29)$$

where ϱ_{kt} is a normalised kernel function. w_{kt} uses a Normal kernel weighting function. ζ_{Tk} gives the rate of convergence and behaves like the bandwidth parameter H in (28), and it is the kernel function that provides greater weight to observations surrounding the parameter estimates at time k relative to more distant observations.

Using a Normal-Wishart prior distribution for $\phi_k | \Sigma_k$ for $k \in \{1, \dots, T\}$:

$$\phi_k | \Sigma_k \sim \mathcal{N}(\phi_{0k}, (\Sigma_k \otimes \Xi_{0k})^{-1}) \quad (30)$$

$$\Sigma_k \sim \mathcal{W}(\alpha_{0k}, \Gamma_{0k}) \quad (31)$$

where ϕ_{0k} is a vector of prior means, Ξ_{0k} is a positive definite matrix, α_{0k} is a scale parameter of the Wishart distribution (\mathcal{W}), and Γ_{0k} is a positive definite matrix.

The prior and weighted likelihood function implies a Normal-Wishart quasi posterior distribution for $\phi_k | \Sigma_k$ for $k = \{1, \dots, T\}$. Formally let $\mathbf{A} = (\bar{x}_1^\top, \dots, \bar{x}_T^\top)^\top$ and $\mathbf{Y} = (x_1, \dots, x_T)^\top$ then:

$$\phi_k | \Sigma_k, \mathbf{A}, \mathbf{Y} \sim \mathcal{N}(\tilde{\theta}_k, (\Sigma_k \otimes \tilde{\Xi}_k)^{-1}) \quad (32)$$

$$\Sigma_k \sim \mathcal{W}(\tilde{\alpha}_k, \tilde{\Gamma}_k^{-1}) \quad (33)$$

with quasi posterior parameters

$$\tilde{\phi}_k = (\mathbf{I}_N \otimes \tilde{\Xi}_k^{-1}) \left[(\mathbf{I}_N \otimes \mathbf{A}' \mathbf{D}_k \mathbf{A}) \hat{\phi}_k + (\mathbf{I}_N \otimes \Xi_{0k}) \phi_{0k} \right] \quad (34)$$

$$\tilde{\Xi}_k = \Xi_{0k} + \mathbf{A}' \mathbf{D}_k \mathbf{A} \quad (35)$$

$$\tilde{\alpha}_k = \alpha_{0k} + \sum_{t=1}^T \varrho_{kt} \quad (36)$$

$$\tilde{\Gamma}_k = \Gamma_{0k} + \mathbf{Y}' \mathbf{D}_k \mathbf{Y} + \Phi_{0k} \Gamma_{0k} \Phi_{0k}' - \tilde{\Phi}_k \tilde{\Gamma}_k \tilde{\Phi}_k^\top \quad (37)$$

where $\hat{\phi}_k = (\mathbf{I}_N \otimes \mathbf{A}' \mathbf{D}_k \mathbf{A})^{-1} (\mathbf{I}_N \otimes \mathbf{A}' \mathbf{D}_k) y$ is the local likelihood estimator for ϕ_k . The matrices Φ_{0k} , $\tilde{\Phi}_k$ are conformable matrices from the vector of prior means, ϕ_{0k} , and a draw from the quasi posterior distribution, $\tilde{\phi}_k$, respectively.

The motivation for employing these methods are threefold. First, we are able to estimate large systems that conventional Bayesian estimation methods do not permit. This is typically because the state-space representation of an N -dimensional TVP VAR (p) requires an additional $N(3/2 + N(p + 1/2))$ state equations for every additional variable. Conventional Markov Chain Monte Carlo (MCMC) methods fail to estimate larger models, which in general confine one to (usually) fewer than 6 variables in the system. Second, the standard approach is fully parametric and requires a law of motion. This can distort inference if the true law of motion is misspecified. Third, the methods used here permit direct estimation of the VAR's time-varying covariance matrix, which has an inverse-Wishart density and is symmetric positive definite at every point in time.

In estimating the model, we use $p=2$ and a Minnesota Normal-Wishart prior with a shrinkage value $\varphi = 0.05$ and centre the coefficient on the first lag of each variable to 0.1 in each respective equation. The prior for the Wishart parameters are set following [Kadiyala and Karlsson \(1997\)](#). For each point in time, we run 500 simulations of the model to generate the (quasi) posterior distribution of parameter estimates. Note we experiment with various lag lengths, $p = \{2, 3, 4, 5\}$; shrinkage values, $\varphi = \{0.01, 0.25, 0.5\}$; and values to centre the coefficient on the first lag of each variable, $\{0, 0.05, 0.2, 0.5\}$. Network measures from these

experiments are qualitatively similar. Notably, adding lags to the VAR and increasing the persistence in the prior value of the first lagged dependent variable in each equation increases computation time.

Appendix E Net and Agg Uncertainty Connectedness Measures

Table F1: \mathcal{C}_{NET} and \mathcal{C}_{AGG} across each business cycle

	Dot com Inv			Dot com Rec			Exp after Dot com			GFC Inv		
	NET	AGG	AGG %	NET	AGG	AGG %	NET	AGG	AGG %	NET	AGG	AGG %
CD	-2.27	20.81	10	0.81	66.58	13.5	-2.04	10.99	8.2	-1.17	12.72	9.4
CM	-3.09	14.28	6.9	-0.26	38.82	7.8	-1.22	11.73	8.8	-0.02	11.85	8.8
CS	-1.02	13.08	6.3	-4.91	47.86	9.7	-0.76	11.38	8.6	-0.72	11.17	8.3
E	-6.24	21.21	10.2	0.37	42.96	8.7	-0.71	12.57	9.4	-2.79	12.54	9.3
F	0.14	18.77	9.1	0.06	66.84	13.5	1.51	16.86	12.7	7.38	23.37	17.3
HC	-1.31	18.31	8.8	-4.11	54.12	11	-0.42	12.24	9.2	-0.21	10.14	7.5
IN	1.79	28.56	13.8	-3.27	62.47	12.6	0.96	13.47	10.1	0.05	12.70	9.4
IT	9.79	36.39	17.6	6.48	68.59	13.9	1.03	12.51	9.4	-0.94	13.79	10.2
M	-0.62	10.64	5.1	-1.47	13.14	2.7	-1.03	9.24	6.9	0.04	9.66	7.1
RE	3.68	16.34	7.9	7.02	24.92	5.1	2.52	13.09	9.8	-1.99	7.67	5.7
U	-0.85	8.71	4.3	-0.67	7.89	1.5	0.17	9.12	6.9	-0.32	9.50	7

	GFC Rec			Exp after GFC			Covid-19 Rec			Total Period		
	NET	AGG	AGG %	NET	AGG	AGG %	NET	AGG	AGG %	NET	AGG	AGG %
CD	-2.98	16.12	6.5	0.07	40.24	12.1	3.64	22.34	10.1	-0.71	29.61	11.1
CM	-2.21	25.37	10.2	3.97	42.58	12.8	1.61	22.46	10.1	1.55	30.49	11.5
CS	1.09	24.50	9.8	-2.33	30.48	9.1	3.36	25.75	11.6	-1.50	24.27	9.1
E	-1.87	23.44	9.4	-0.16	37.61	11.2	0.22	25.71	11.6	-0.80	28.27	10.6
F	8.61	40.32	16.2	-1.58	19.17	5.8	-8.63	14.51	6.5	0.54	22.15	8.3
HC	-1.81	20.04	8	-0.17	35.02	10.5	-0.53	14.94	6.7	-0.56	26.45	9.9
IN	3.41	33.15	13.3	-0.43	39.94	12.0	-0.77	24.64	11.1	0.17	31.47	11.9
IT	-1.46	25.93	10.5	2.84	44.45	13.3	3.30	24.71	11.5	2.23	33.71	12.7
M	-0.79	15.93	6.2	-0.99	20.01	5.9	-3.06	19.40	8.7	-0.98	15.84	6.0
RE	-0.89	14.47	5.8	-0.55	14.68	4.4	-1.48	12.14	5.4	0.51	14.22	5.3
U	-1.09	10.27	4.1	-0.66	9.70	2.9	2.33	14.97	6.7	-0.43	9.59	3.6

Notes: The table shows the average NET and AGG network characteristics with respect to the 11 U.S. industries. When the NET measure is positive the $IVIX^{(I)}$ can be classified as a NET marginal transmitter, while, when negative, it can be classified as a NET marginal receiver. The AGG statistic is computed as the sum (in absolute values) between TO and FROM. The highest values of the AGG statistic are associated with uncertainty hubs, while the lowest with uncertainty non-hubs. The statistics are reported for each business cycle in our sample, namely inversion, recession, expansion separately and also for the total period, namely from 03-01-2000 to 29-05-2020, at a daily frequency.

Appendix F Robustness Checks

Table F1: ADS Predictive Results

Panel A: ADS					
	$h=1$	$h=3$	$h=6$	$h=9$	$h=12$
$\mathcal{C}_t \mid X_t$	-0.020 (0.016)	-0.032* (0.019)	-0.036** (0.019)	-0.055*** (0.017)	-0.038** (0.019)
Adj. R^2	0.273	0.030	0.029	0.063	0.072
Obs	243	241	238	235	232
Panel B: ADS Expansion					
	$h=1$	$h=3$	$h=6$	$h=9$	$h=12$
$\mathcal{C}_t \mid X_t$	-0.002 (0.003)	-0.003 (0.003)	-0.005* (0.003)	-0.007*** (0.003)	-0.007*** (0.003)
Adj. R^2	0.009	0.055	0.065	0.082	0.056
Obs	243	241	238	235	232
Panel C: ADS Recession					
	$h=1$	$h=3$	$h=6$	$h=9$	$h=12$
$\mathcal{C}_t \mid X_t$	-0.022 (0.016)	-0.025 (0.019)	-0.031* (0.019)	-0.048*** (0.019)	-0.031* (0.019)
Adj. R^2	0.273	0.022	0.025	0.053	0.067
Obs	243	241	238	235	232

Notes: This table presents the results of the predictive regression in equation 9 between the aggregate network connectedness and the 3-month moving average of the ADS indicator of business cycle (Panel A). In Panel B and Panel C the results of the predictive regression with respect to the ADS expansion and recession indicators are reported, respectively. We also add a set of controls, X . The five columns of the table represent different predictability horizons with $h \in (1, 3, 6, 9, 12)$. Regressions' coefficients and standard errors (in parentheses), and adjusted- R^2 are reported. Coefficients are marked with *, **, *** for 10%, 5%, 1% significance levels, respectively. Intercept and controls results are not reported for the sake of space. Series are considered at monthly frequency between 01-2000 and 05-2020.

Table F2: ADS Predictive Results

Panel A: IP Growth Rate					
	$h=1$	$h=3$	$h=6$	$h=9$	$h=12$
$\mathcal{C}_t \mid X_t$	-0.001 (0.001)	-0.003** (0.001)	-0.003** (0.001)	-0.003*** (0.001)	-0.003** (0.001)
Adj. R^2	0.247	0.054	0.035	0.057	0.062
Obs	243	241	238	235	232

Panel B: USCI Growth Rate					
	$h=1$	$h=3$	$h=6$	$h=9$	$h=12$
$\mathcal{C}_t \mid X_t$	-0.019 (0.027)	-0.060** (0.029)	-0.087*** (0.030)	-0.150*** (0.027)	-0.140*** (0.026)
Adj. R^2	0.009	0.055	0.065	0.082	0.056
Obs	0.205	0.078	0.058	0.213	0.280

Notes: This table presents the results of the predictive regression in equation 9 between the aggregate network connectedness, and the industrial production growth rate in Panel A, and the US coincident indicator in Panel B. We also add a set of controls, X . The five columns of the table represent different predictability horizons with $h \in (1, 3, 6, 9, 12)$. Regressions' coefficients and standard errors (in parentheses), and adjusted- R^2 are reported. Coefficients are marked with *, **, *** for 10%, 5%, 1% significance levels, respectively. Intercept and controls results are not reported for the sake of space. Series are considered at monthly frequency between 01-2000 and 05-2020.

Table F3: Coincident Indicators Predictive Results (2)

Dependent: CFNAI-3M					
	$h=1$	$h=3$	$h=6$	$h=9$	$h=12$
$\mathcal{C}_t \mid X_t$	-0.008** (0.004)	-0.021*** (0.007)	-0.023*** (0.007)	-0.039*** (0.007)	-0.028*** (0.007)
USCI	0.104*** (0.006)	0.064*** (0.010)	0.044*** (0.011)	0.025** (0.011)	0.003 (0.011)
Adj. R^2	0.678	0.280	0.123	0.191	0.164
Obs	243	241	238	235	232

Dependent: ADS					
	$h=1$	$h=3$	$h=6$	$h=9$	$h=12$
$\mathcal{C}_t \mid X_t$	-0.012 (0.014)	-0.023 (0.018)	-0.033** (0.019)	-0.052*** (0.019)	-0.037** (0.019)
USCI	0.172*** (0.020)	0.088*** (0.029)	0.059** (0.029)	0.041 (0.029)	0.023 (0.029)
Adj. R^2	0.440	0.064	0.042	0.068	0.071
Obs	243	241	238	235	232

Notes: This table presents the results of the predictive regressions between the aggregate network connectedness, and the coincident indicators of business cycle, namely CFNAI and ADS. We present results for regression equation 9 in which we add a set of controls including also the leading indicator, USLI. The five columns of the table represent different predictability horizons with $h \in (1, 3, 6, 9, 12)$. Regressions' coefficients and standard errors (in parentheses), and adjusted- R^2 are reported. Coefficients are marked with *, **, *** for 10%, 5%, 1% significance levels, respectively. Intercept and controls results are not reported for the sake of space, exception for the USLI control. Series are considered at monthly frequency between 01-2000 and 05-2020.

Table F4: ADS Hubs Network Predictive Results

Panel A: ADS					
	$h=1$	$h=3$	$h=6$	$h=9$	$h=12$
$\mathcal{C}_t^{\text{hub}}$	-0.029*** (0.008)	-0.022** (0.008)	-0.018** (0.009)	-0.019** (0.009)	-0.014 (0.009)
Adj. R^2	0.044	0.023	0.014	0.016	0.007
Obs	244	242	239	236	233
$\mathcal{C}_t^{\text{hub}} X_t$	-0.010 (0.009)	-0.022** (0.011)	-0.025** (0.011)	-0.031*** (0.011)	-0.025** (0.011)
Adj. R^2	0.271	0.038	0.037	0.063	0.078
Obs	243	241	238	235	232
Panel B: ADS Expansion					
	$h=1$	$h=3$	$h=6$	$h=9$	$h=12$
$\mathcal{C}_t^{\text{hub}}$	-0.001 (0.001)	-0.002* (0.001)	-0.001 (0.001)	-0.003** (0.001)	-0.004*** (0.001)
Adj. R^2	0.004	0.006	0.0003	0.021	0.032
Obs	244	242	239	236	233
$\mathcal{C}_t^{\text{hub}} X_t$	0.001 (0.002)	-0.001 (0.001)	-0.001 (0.001)	-0.003** (0.001)	-0.005*** (0.001)
Adj. R^2	0.010	0.052	0.054	0.075	0.073
Obs	243	241	238	235	232
Panel C: ADS Recession					
	$h=1$	$h=3$	$h=6$	$h=9$	$h=12$
$\mathcal{C}_t^{\text{hub}}$	-0.029*** (0.008)	-0.020** (0.008)	-0.017* (0.009)	-0.016* (0.009)	-0.011 (0.009)
Adj. R^2	0.044	0.018	0.012	0.010	0.002
Obs	244	242	239	236	233
$\mathcal{C}_t^{\text{hub}} X_t$	-0.011 (0.009)	-0.021* (0.011)	-0.024** (0.011)	-0.028*** (0.011)	-0.020* (0.011)
Adj. R^2	0.271	0.030	0.035	0.054	0.070
Obs	243	241	238	235	232

Notes: This table presents the results of the predictive regressions between the uncertainty hubs sub-network and the ADS Index, indicator of business cycle (Panel A). In Panel B and Panel C the results of the predictive regression with respect to the ADS expansion and recession indicators are reported, respectively. We present results for both regression equations 10 and ?? in which we add a set of controls. The five columns of the table represent different predictability horizons with $h \in (1, 3, 6, 9, 12)$. Regressions' coefficients and standard errors (in parentheses), and adjusted- R^2 are reported. Coefficients are marked with *, **, *** for 10%, 5%, 1% significance levels, respectively. Intercept and controls results are not reported for the sake of space. Series are considered at monthly frequency between 01-2000 and 05-2020.

Appendix G Predicting the US GDP and its volatility

Table F1: US GDP Predictive Results

Panel A: GDP Growth Rate				
	$h=1$	$h=2$	$h=3$	$h=4$
$C_t \mid X_t$	-0.056 (0.046)	-0.158*** (0.041)	-0.176*** (0.041)	-0.156*** (0.041)
Adj. R^2	0.015	0.221	0.218	0.250
Obs	79	78	77	76
Panel B: GDP Volatility				
	$h=1$	$h=2$	$h=3$	$h=4$
$C_t \mid X_t$	0.028* (0.014)	0.036** (0.014)	0.047*** (0.014)	0.039*** (0.013)
Adj. R^2	0.138	0.106	0.165	0.219
Obs	79	78	77	76

Notes: This table presents the results of the predictive regression 9 between the aggregate network connectedness, and the US GDP growth rate (Panel A) and GDP volatility (Panel B). The four columns of the table represent different predictability horizons with $h \in (1, 2, 3, 4)$ quarters. Regressions' coefficients and standard errors (in parentheses), and adjusted- R^2 are reported. Coefficients are marked with *, **, *** for 10%, 5%, 1% significance levels, respectively. Intercept and controls results are not reported for the sake of space. Series are all taken at quarterly frequency, between 01-2000 and 05-2020.

Appendix H Hubs and non-hubs predictive results

Table F1: CFNAI-MA3 Hubs Network Predictive Results

Panel A: CFNAI-MA3					
	$h=1$	$h=3$	$h=6$	$h=9$	$h=12$
$\mathcal{C}_t^{\text{hub}} X_t$	-0.009** (0.004)	-0.016*** (0.004)	-0.019*** (0.004)	-0.023*** (0.004)	-0.018*** (0.004)
Adj. R^2	0.302	0.176	0.104	0.178	0.186
Obs	243	241	238	235	232
Panel B: CFNAI-MA3 Expansion					
	$h=1$	$h=3$	$h=6$	$h=9$	$h=12$
$\mathcal{C}_t^{\text{hub}} X_t$	-0.004*** (0.001)	-0.005*** (0.001)	-0.006*** (0.001)	-0.006*** (0.001)	-0.006*** (0.001)
Adj. R^2	0.099	0.152	0.238	0.290	0.289
Obs	243	241	238	235	232
Panel C: CFNAI-MA3 Recession					
	$h=1$	$h=3$	$h=6$	$h=9$	$h=12$
$\mathcal{C}_t^{\text{hub}} X_t$	-0.005 (0.003)	-0.012*** (0.004)	-0.013*** (0.004)	-0.017*** (0.004)	-0.012*** (0.004)
Adj. R^2	0.291	0.153	0.087	0.148	0.153
Obs	243	241	238	235	232

Notes: This table presents the results of the predictive regressions ?? between the uncertainty hubs sub-network and the 3-month moving average of the Chicago FED National Activity Index (CFNAI-MA3), indicator of business cycle (Panel A). In Panel B and Panel C the results of the predictive regression with respect to the CFNAI-MA3 expansion and recession indicators are reported, respectively. The five columns of the table represent different predictability horizons with $h \in (1, 3, 6, 9, 12)$. Regressions' coefficients and standard errors (in parentheses), and adjusted- R^2 are reported. Coefficients are marked with *, **, *** for 10%, 5%, 1% significance levels, respectively. Intercept and controls results are not reported for the sake of space. Series are considered at monthly frequency between 01-2000 and 05-2020.

Table F2: Stricter Hubs vs no-Hubs Network Predictive Results

Panel A: CFNAI-MA3					
	$h=1$	$h=3$	$h=6$	$h=9$	$h=12$
$\mathcal{C}_t^{\text{hub}} X_t$	-0.010*** (0.003)	-0.013*** (0.004)	-0.016*** (0.004)	-0.017*** (0.004)	-0.016*** (0.004)
$\mathcal{C}_t^{\text{non-hub}} X_t$	-0.014** (0.006)	-0.022*** (0.006)	-0.015** (0.007)	-0.013* (0.007)	-0.0003 (0.007)
Adj. R^2	0.334	0.224	0.121	0.163	0.173
Obs	243	241	238	235	232
Panel B: CFNAI-MA3 Expansion					
	$h=1$	$h=3$	$h=6$	$h=9$	$h=12$
$\mathcal{C}_t^{\text{hub}} X_t$	-0.003** (0.001)	-0.004*** (0.001)	-0.004*** (0.001)	-0.005*** (0.001)	-0.006*** (0.001)
$\mathcal{C}_t^{\text{non-hub}} X_t$	0.0004 (0.002)	-0.002 (0.002)	-0.005*** (0.002)	-0.002 (0.002)	-0.0002 (0.002)
Adj. R^2	0.073	0.135	0.240	0.297	0.293
Obs	243	241	238	235	232
Panel C: CFNAI-MA3 Recession					
	$h=1$	$h=3$	$h=6$	$h=9$	$h=12$
$\mathcal{C}_t^{\text{hub}} X_t$	-0.007** (0.003)	-0.010*** (0.004)	-0.012*** (0.004)	-0.012*** (0.004)	-0.010*** (0.004)
$\mathcal{C}_t^{\text{non-hub}} X_t$	-0.015*** (0.005)	-0.020*** (0.006)	-0.009 (0.006)	-0.012* (0.006)	-0.0002 (0.006)
Adj. R^2	0.326	0.200	0.098	0.135	0.141
Obs	243	241	238	235	232
Panel D: CLI					
	$h=1$	$h=3$	$h=6$	$h=9$	$h=12$
$\mathcal{C}_t^{\text{hub}} X_t$	-0.013** (0.005)	-0.024*** (0.006)	-0.038*** (0.006)	-0.048*** (0.006)	-0.050*** (0.006)
$\mathcal{C}_t^{\text{non-hub}} X_t$	-0.010 (0.008)	-0.017* (0.009)	-0.019* (0.010)	-0.022** (0.010)	-0.011 (0.010)
Adj. R^2	0.451	0.341	0.285	0.338	0.334
Obs	243	241	238	235	232
Panel E: CFNAI-MA3 controlling for CLI					
	$h=1$	$h=3$	$h=6$	$h=9$	$h=12$
$\mathcal{C}_t^{\text{hub}} X_t$	-0.006** (0.003)	-0.010*** (0.003)	-0.014*** (0.004)	-0.016*** (0.004)	-0.016*** (0.004)
$\mathcal{C}_t^{\text{non-hub}} X_t$	-0.013*** (0.004)	-0.022*** (0.005)	-0.015** (0.006)	-0.013* (0.006)	-0.0003 (0.007)
CLI	0.418*** (0.036)	0.336*** (0.051)	0.241*** (0.052)	0.112** (0.053)	-0.017
Adj. R^2	0.579	0.378	0.197	0.177	0.170
Obs	243	241	238	235	232

Notes: This table presents the results of the predictive regression 10 comparing the predictive ability of the uncertainty hubs vs non-hubs sub-networks, with respect to the 3-month moving average of the Chicago FED National Activity Index (CFNAI-MA3) in Panel A. In Panel B and Panel C the results of the predictive regression with respect to the CFNAI expansion and recession periods are reported, respectively. In Panel D the results with respect to the leading indicator CLI are reported. In Panel E the results of predicting the coincident business cycle indicator controlling for CLI are reported. The five columns of the table represent different predictability horizons with $h \in (1, 3, 6, 9, 12)$. Regressions' coefficients and standard errors (in parentheses), and adjusted- R^2 are reported. Coefficients are marked with *, **, *** for 10%, 5%, 1% significance levels, respectively. Intercept and controls results are not reported for the sake of space, the only exception being the CLI control. Series are considered at monthly frequency between 01-2000 and 05-2020.

Table F3: US GDP Prediction with Hubs and non-Hubs

Panel A: GDP Growth Rate					
		$h=1$	$h=2$	$h=3$	$h=4$
$\mathcal{C}_t^{\text{hub}}$		-0.055**	-0.083***	-0.104***	-0.081***
	(0.027)	(0.024)	(0.024)	(0.024)	
$\mathcal{C}_t^{\text{non-hub}}$		0.017	-0.043	-0.017	-0.039
	(0.044)	(0.039)	(0.039)	(0.039)	
Adj. R^2		0.038	0.223	0.238	0.246
Obs		79	78	77	76
Panel B: GDP Volatility					
		$h=1$	$h=2$	$h=3$	$h=4$
$\mathcal{C}_t^{\text{hub}}$		0.030***	0.029***	0.024***	0.015*
		(0.008)	(0.008)	(0.008)	(0.008)
$\mathcal{C}_t^{\text{non-hub}}$		-0.016	-0.004	0.014	0.024*
		(0.013)	(0.013)	(0.013)	(0.013)
Adj. R^2		0.236	0.166	0.170	0.221
Obs		79	78	77	76

Notes: This table presents the results of the predictive regression 9 between the hubs and non-hubs networks, and the US GDP growth rate (Panel A) and GDP volatility (Panel B). The four columns of the table represent different predictability horizons with $h \in (1, 2, 3, 4)$ quarters. Regressions' coefficients and standard errors (in parentheses), and adjusted- R^2 are reported. Coefficients are marked with *, **, *** for 10%, 5%, 1% significance levels, respectively. Intercept and controls results are not reported for the sake of space. Series are all taken at quarterly frequency, between 01-2000 and 05-2020.